A study of meson and baryon decays to strange final states with GlueX in Hall D

(A proposal to the 39th Jefferson Lab Program Advisory Committee)

M. Dugger,[1] B. Ritchie,[1] E. Anassontzis,[2] P. Ioannou,[2] C. Kourkoumeli,[2] G. Voulgaris,[2] N. Jarvis,[3] W. Levine,[3] P. Mattione,[3] C. A. Meyer,[3,*] R. Schumacher,[3] P. Collins,[4] F. Klein,[4] D. Sober,[4] D. Doughty,[5] A. Barnes,[6] R. Jones,[6] J. McIntyre,[6] F. Mokaya,[6] B. Pratt,[6] I. Senderovich,[6] W. Boeglin,[7] L. Guo,[7] P. Khetarpal,[7] E. Pooser,[7] J. Reinhold,[7] H. Al Ghoul,[8] S. Capstick,[8] V. Crede,[8] P. Eugenio,[8] A. Ostrovidov,[8] N. Sparks,[8] A. Tsaris,[8] D. Ireland,[9] K. Livingston,[9] D. Bennett,[10] J. Bennett,[10] J. Frye,[10] J. Leckey,[10] R. Mitchell,[10] K. Moriya,[10] M. R. Shepherd,[10,†] A. Szczepaniak,[10] R. Miskimen,[11] M. Williams,[12] P. Ambrozewicz,[13] A. Gasparian,[13] R. Pedroni,[13] T. Black,[14] L. Gan,[14] J. Dudek,[15,16] F. Close,[17] E. Swanson,[18] S. Denisov,[19] G. Huber,[20] S. Katsaganis,[20] D. Kolybaba,[20] G. Lolos,[20] Z. Papandreou,[20] A. Semenov,[20] I. Semenova,[20] M. Tahani,[20] W. Brooks,[21] S. Kuleshov,[21] A. Toro,[21] F. Barbosa,[16] E. Chudakov,[16,‡] H. Egiyan,[16] M. Ito,[16] D. Lawrence,[16] L. Pentchev,[16] Y. Qiang,[16] E. S. Smith,[16] A. Somov,[16] S. Taylor,[16] T. Whitlatch,[16] E. Wolin,[16] and B. Zihlmann[16]

(The GlueX Collaboration)

[1] *Arizona State University, Tempe, Arizona 85287, USA*
[2] *University of Athens, GR-10680 Athens, Greece*
[3] *Carnegie Mellon University, Pittsburgh, Pennsylvania 15213, USA*
[4] *Catholic University of America, Washington, D.C. 20064, USA*
[5] *Christopher Newport University, Newport News, Virginia 23606, USA*
[6] *University of Connecticut, Storrs, Connecticut 06269, USA*
[7] *Florida International University, Miami, Florida 33199, USA*
[8] *Florida State University, Tallahassee, Florida 32306, USA*
[9] *University of Glasgow, Glasgow G12 8QQ, United Kingdom*
[10] *Indiana University, Bloomington, Indiana 47405, USA*
[11] *University of Massachusetts, Amherst, Massachusetts 01003, USA*
[12] *Massachusetts Institute of Technology, Cambridge, Massachusetts 02139, USA*
[13] *North Carolina A&T State University, Greensboro, North Carolina 27411, USA*
[14] *University of North Carolina, Wilmington, North Carolina 28403, USA*
[15] *Old Dominion University, Norfolk, Virginia 23529, USA*
[16] *Thomas Jefferson National Accelerator Facility, Newport News, Virginia 23606, USA*
[17] *University of Oxford, Oxford OX1 3NP, United Kingdom*
[18] *University of Pittsburgh, Pittsburgh, Pennsylvania 15260, USA*
[19] *Institute for High Energy Physics, Protvino, Russia*
[20] *University of Regina, Regina, SK S4S 0A2, Canada*
[21] *Universidad Técnica Federico Santa María, Casilla 110-V Valparaíso, Chile*

(Dated: May 3, 2012)

The primary motivation of the GlueX experiment is to search for and ultimately study the pattern of gluonic excitations in the meson spectrum produced in γp collisions. Recent lattice QCD calculations predict a rich spectrum of hybrid mesons that have both exotic and non-exotic J^{PC}, corresponding to $q\bar{q}$ ($q = u$, d, or s) states coupled with a gluonic field. A thorough study of the hybrid spectrum, including the identification of the isovector triplet, with charges 0 and ± 1, and both isoscalar members, $|s\bar{s}\rangle$ and $|u\bar{u}\rangle + |d\bar{d}\rangle$, for each predicted hybrid combination of J^{PC}, may only be achieved by conducting a systematic amplitude analysis of many different hadronic final states. We propose the development of a kaon identification system, supplementing the existing GlueX forward time-of-flight detector, in order to cleanly select meson and baryon decay channels that include kaons. Once this detector has been installed and commissioned, we plan to collect a total of 200 days of physics analysis data at an average intensity of 5×10^7 tagged photons on target per second. This data sample will provide an order of magnitude statistical improvement over the initial GlueX data set and, with the developed kaon identification system, a significant increase in the potential for GlueX to make key experimental advances in our knowledge of hybrid mesons and Ξ baryons.

I. INTRODUCTION AND BACKGROUND

A long-standing goal of hadron physics has been to understand how the quark and gluonic degrees of freedom that are present in the fundamental QCD Lagrangian manifest themselves in the spectrum of hadrons. Of

* Spokesperson
† Deputy Spokesperson
‡ Hall D Leader

particular interest is how the gluon-gluon interactions might give rise to physical states with gluonic excitations. One class of such states is the hybrid mesons, which can be naively thought of as quark anti-quark pairs coupled to a valence gluon ($q\bar{q}g$). Recent lattice QCD calculations [1] predict a rich spectrum of hybrid mesons. A subset of these hybrids have an unmistakable experimental signature: angular momentum (J), parity (P), and charge conjugation (C) that cannot be created from just a quark-antiquark pair. Such states are called exotic hybrid mesons. The primary goal of the GlueX experiment in Hall D is to search for and study these mesons.

A detailed overview of the motivation for the GlueX experiment as well as the design of the detector and beamline can be found in the initial proposal to the Jefferson Lab Program Advisory Committee (PAC) 30 [2] and a subsequent PAC 36 update [3]. While the currently-approved 120 days of beam time with the baseline detector configuration will allow GlueX an unprecedented opportunity to search for exotic hybrid mesons, the existing baseline design is inadequate for studying mesons or baryons with strange quarks. This proposal focuses on developing additional detector capability that will allow GlueX to identify kaons and operate at high intensity. This functionality is essential in order for the GlueX experiment to pursue its primary goal of solidifying our experimental understanding of hybrids by identifying *patterns* of hybrid mesons, both isoscalar and isovector, exotic and non-exotic, that are embedded in the spectrum of conventional mesons.

A. Theoretical context

Our understanding of how gluonic excitations manifest themselves within QCD is maturing thanks to recent results from lattice QCD. This numerical approach to QCD considers the theory on a finite, discrete grid of points in a manner that would become exact if the lattice spacing were taken to zero and the spatial extent of the calculation, *i.e.,* the "box size," was made large. In practice, rather fine spacings and large boxes are used so that the systematic effect of this approximation should be small. The main limitation of these calculations at present is the poor scaling of the numerical algorithms with decreasing quark mass - in practice most contemporary calculations use a range of artificially heavy light quarks and attempt to observe a trend as the light quark mass is reduced toward the physical value. Trial calculations at the physical quark mass have begun and regular usage is anticipated within a few years.

The spectrum of eigenstates of QCD can be extracted from correlation functions of the type $\langle 0|\mathcal{O}_f(t)\mathcal{O}_i^\dagger(0)|0\rangle$, where the $\mathcal{O}^\dagger$ are composite QCD operators capable of interpolating a meson or baryon state from the vacuum. The time-evolution of the Euclidean correlator indicates the mass spectrum ($e^{-m_{\mathfrak{n}}t}$) and information about quark-gluon substructure can be inferred from matrix-elements $\langle \mathfrak{n}|\mathcal{O}^\dagger|0\rangle$. In a series of recent papers [4–7], the Hadron Spectrum Collaboration has explored the spectrum of mesons and baryons using a large basis of composite QCD interpolating fields, extracting a spectrum of states of determined $J^{P(C)}$, including states of high internal excitation.

As shown in Fig. 1, these calculations, for the first time, show a clear and detailed spectrum of exotic J^{PC} mesons, with a lightest 1^{-+} lying a few hundred MeV below a 0^{+-} and two 2^{+-} states. Beyond this, through analysis of the matrix elements $\langle \mathfrak{n}|\mathcal{O}^\dagger|0\rangle$ for a range of different quark-gluon constructions, $\mathcal{O}$, we can infer [1] that although the bulk of the non-exotic J^{PC} spectrum has the expected systematics of a $q\bar{q}$ bound state system, some states are only interpolated strongly by operators featuring non-trivial gluonic constructions. One may interpret these states as non-exotic hybrid mesons, and, by combining them with the spectrum of exotics, it is then possible to isolate a lightest hybrid supermultiplet of $(0,1,2)^{-+}$ and 1^{--} states, roughly 1.3 GeV heavier than the ρ meson. The form of the operator that has strongest overlap onto these states has an S-wave $q\bar{q}$ pair in a color octet configuration and an exotic gluonic field in a color octet with $J_g^{P_g C_g} = 1^{+-}$, a *chromomagnetic* configuration. The heavier $(0,2)^{+-}$ states, along with some positive parity non-exotic states, appear to correspond to a P-wave coupling of the $q\bar{q}$ pair to the same chromomagnetic gluonic excitation.

A similar calculation for isoscalar states uses both $u\bar{u}+d\bar{d}$ and $s\bar{s}$ constructions and is able to extract both the spectrum of states and also their hidden flavor mixing. (See Fig. 1.) The basic experimental pattern of significant mixing in 0^{-+} and 1^{++} channels and small mixing elsewhere is reproduced, and, for the first time, we are able to say something about the degree of mixing for exotic-J^{PC} states. In order to probe this mixing experimentally, it is essential to be able to reconstruct decays to both strange and non-strange final state hadrons.

A chromomagnetic gluonic excitation can also play a role in the spectrum of baryons: constructions beyond the simple qqq picture can occur when three quarks are placed in a color octet coupled to the chromomagnetic excitation. The baryon sector offers no "smoking gun" signature for hybrid states, as all J^P can be accessed by three quarks alone, but lattice calculations [7] indicate that there are "excess" nucleons with $J^P = 1/2^+,\ 3/2^+,\ 5/2^+$ and excess Δ's with $J^P = 1/2^+, 3/2^+$ that have a hybrid component. An interesting observation that follows from this study is that there appears to be a common energy cost for the chromomagnetic excitation, regardless of whether it is in a meson or baryon. In Fig. 2 we show the hybrid meson spectrum alongside the hybrid baryon spectrum with the quark mass contribution subtracted (approximately, by subtracting the ρ mass from the mesons, and the nucleon mass from the baryons). We see that there appears to be a common scale $\sim$ 1.3 GeV for the gluonic excitation, which does not vary significantly with varying quark mass.

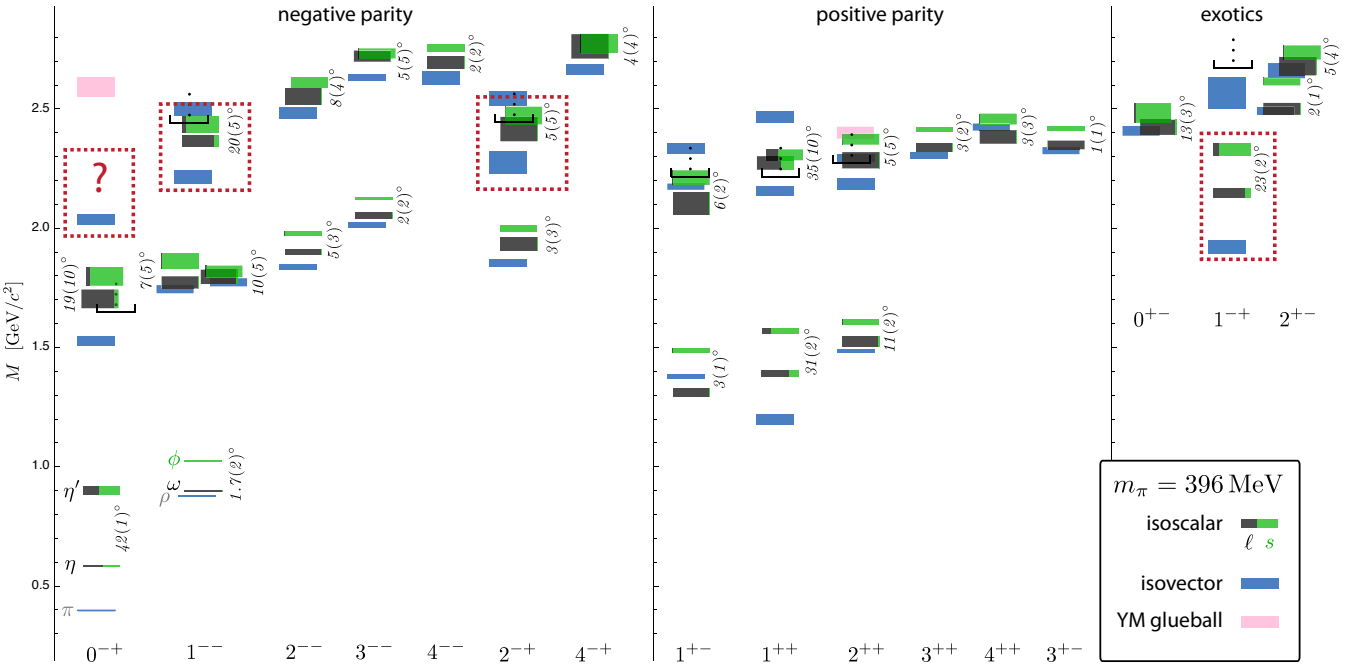

FIG. 1. A compilation of recent lattice QCD computations for both the isoscalar and isovector light mesons from Ref. [1], including $\ell\bar{\ell}$ $\left(|\ell\bar{\ell}\rangle \equiv (|u\bar{u}\rangle + |d\bar{d}\rangle)/\sqrt{2}\right)$ and $s\bar{s}$ mixing angles (indicated in degrees). The dynamical computation is carried out with two flavors of quarks, light (ℓ) and strange (s). The s quark mass parameter is tuned to match physical $s\bar{s}$ masses, while the light quark mass parameters are heavier, giving a pion mass of 396 MeV. The black brackets with upward ellipses represent regions of the spectrum where present techniques make it difficult to extract additional states. The dotted boxes indicate states that are interpreted as the lightest hybrid multiplet – the extraction of clear 0^{-+} states in this region is difficult in practice.

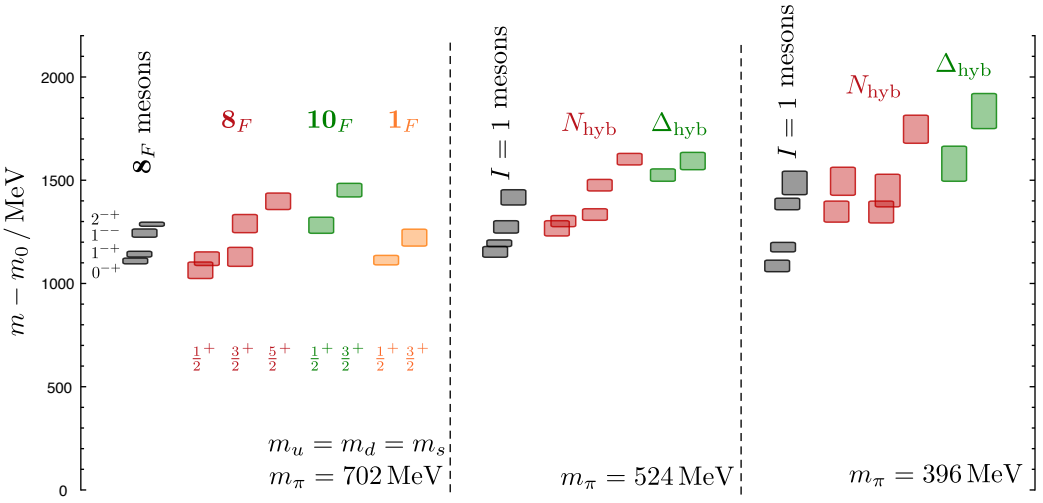

FIG. 2. Spectrum of gluonic excitations in hybrid mesons (grey) and hybrid baryons (red, green, and orange) for three light quark masses. The mass scale is $m - m_\rho$ for mesons and $m - m_N$ for baryons to approximately subtract the effect of differing numbers of quarks. The left calculation is performed with perfect $SU(3)$-flavor symmetry, and hybrid members of the flavor octets (8_F), decuplet (10_F), and singlet (1_F) are shown. The middle and right calculations are performed with a physical $s\bar{s}$ mass and two different values of m_π.

Hybrid baryons will be challenging to extract experimentally because they lack "exotic" character, and can only manifest themselves by overpopulating the predicted spectrum with respect to a particular model. The current experimental situation of nucleon and Δ excitations is, however, quite contrary to the findings in the meson sector. Fewer baryon resonances are observed than are expected from models using three symmetric quark degrees of freedom, which does not encourage adding additional gluonic degrees of freedom. The current experimental efforts at Jefferson Lab aim to identify the relevant degrees of freedom which give rise to nucleon excitations.

While lattice calculations have made great progress at predicting the N^* and Δ spectrum, including hybrid baryons [7, 8], calculations are also underway for Ξ and Ω resonances. The properties of these multi-strange states are poorly known; only the J^P of the $\Xi(1820)$ have been (directly) determined experimentally [9]. Previous experiments searching for Cascades were limited by low statistics and poor detector acceptance, making the interpretation of available data difficult. An experimental program on Cascade physics using the GlueX detector provides a new window of opportunity in hadron spectroscopy and serves as a complementary approach to the challenging study of broad and overlapping N^* states. Furthermore, multi-strange baryons provide an important missing link between the light-flavor and the heavy-flavor baryons. Just recently many new beautiful baryons, Σ_b^-, Ξ_b^-, Ω_b^-, have been discovered at the Tevatron [10–14]. We discuss Ξ baryons further in Section IV.

B. Experimental context

GlueX is ideally positioned to conduct a search for light quark exotics and provide complementary data on the spectrum of light quark mesons. It is anticipated that between now and the time GlueX begins data taking, many results on the light quark spectrum will have emerged from the BESIII experiment, which is currently attempting to collect about 10^8 to 10^9 J/ψ and ψ' decays. These charmonium states decay primarily through $c\bar{c}$ annihilation and subsequent hadronization into light mesons, making them an ideal place to study the spectrum of light mesons. In fact several new states have already been reported by the BESIII collaboration such as the $X(1835)$, $X(2120)$, and $X(2370)$ in $J/\psi \to \gamma X$, $X \to \eta'\pi\pi$ [15]. No quantum number assignment for these states has been made yet, so it is not yet clear where they fit into the meson spectrum. GlueX can provide independent confirmation of the existence of these states in a completely different production mode, in addition to measuring (or confirming) their J^{PC} quantum numbers. This will be essential for establishing the location of these states in the meson spectrum. The BESIII experiment has the ability to reconstruct virtually any combination of final state hadrons, and, due to the well-known initial state, kinematic fitting can be used to virtually eliminate background. The list of putative new states and, therefore, the list of channels to explore with GlueX, is only expected to grow over the next few years as BESIII acquires and analyzes its large samples of charmonium data.

While the glue-rich $c\bar{c}$ decays of charmonium have long been hypothesized as the ideal place to look for glueballs, decays of charmonium have also recently been used to search for exotics. The CLEO-c collaboration studied both $\pi^+\pi^-$ and $\eta'\pi^\pm$ resonances in the decays of $\chi_{c1} \to \eta'\pi^+\pi^-$ and observed a significant signal for an exotic 1^{-+} amplitude in the $\eta'\pi^\pm$ system [16]. The observation is consistent with the $\pi_1(1600)$ previously reported by E852 in the $\eta'\pi$ system [17]. However, unlike E852, the CLEO-c analysis was unable to perform a model-independent extraction of the $\eta'\pi$ scattering amplitude and phase to validate the resonant nature of the 1^{-+} amplitude. A similar analysis of χ_{c1} decays will most likely be performed by BESIII; however, even with an order of magnitude more data, the final $\eta'\pi^+\pi^-$ sample is expected to be just tens of thousands of events, significantly less than the proposed samples that will be collected with GlueX. With the exception of this recent result from CLEO-c, the picture in the light quark exotic sector, and the justification for building GlueX, remains largely the same as it did at the time of the original GlueX proposal; see Ref. [18] for a review. All exotic candidates reported to date are isovector 1^{-+} states (π_1). With the addition of kaon identification, GlueX is capable of exploring all possible decay modes (non-strange and strange) in order to establish not just one exotic state, but a *pattern* of hybrid states with both exotic and non-exotic quantum numbers.

The idea that hybrids should also appear as supernumerary states in the spectrum of non-exotic J^{PC} mesons suggests an interesting interpretation of recent data in charmonium. Three independent experiments have observed a state denoted $Y(4260)$ [19–22]; it has 1^{--} quantum numbers but has no clear assignment in the arguably well-understood spectrum of $c\bar{c}$. Even though the state is above $D\bar{D}$ threshold, it does not decay strongly to $D\bar{D}$ as the other 1^{--} $c\bar{c}$ states in that region do. Its mass is about 1.2 GeV above the ground state J/ψ, which is similar to the splitting observed in lattice calculations of light mesons and baryons. If this state is a non-exotic hybrid, an obvious, but very challenging, experimental goal would be to identify the exotic 1^{-+} $c\bar{c}$ hybrid member of the same multiplet, which should have approximately the same mass[1]. It is not clear how to produce such a state with existing experiments. In the light quark sector, some have suggested that the recently discovered

[1] Like the light quark mesons discussed in Sec. I A, the expectation in charmonium is that a 1^{--} non-exotic hybrid would exist with about the same mass as the 1^{-+} exotic charmonium hybrid [23, 24].

$Y(2175)$ [25–27] is the strangeonium ($s\bar{s}$) analogue of the $Y(4260)$. If this is true, GlueX is well-positioned to study this state and search for its exotic counterpart. We discuss this further in Section III B.

Recent CLAS results [28, 29] also suggest many opportunities to make advances in baryon spectroscopy. The CLAS collaboration investigated Cascade photoproduction in the reactions $\gamma p \to K^+K^+(X)$ as well as $\gamma p \to K^+K^+\pi^-(X)$ and among other things, determined the mass splitting of the ground state (Ξ^-, Ξ^0) doublet to be 5.4 ± 1.8 MeV/c^2, which is consistent with previous measurements. Moreover, the differential (total) cross sections for the Ξ^- have been determined in the photon energy range from 2.75 to 3.85 GeV [29]. The cross section results are consistent with a production mechanism of $Y^* \to \Xi^- K^+$ through a t-channel process. The reaction $\gamma p \to K^+K^+\pi^-[\Xi^0]$ was also studied in search of excited Cascade resonances, but no significant signal for an excited Cascade state, other than the $\Xi^-(1530)$, was observed. The absence of higher-mass signals is very likely due to the low photon energies and the limited acceptance of the CLAS detector. Equipped with a kaon identification system, the GlueX experiment will be well-suited to search for and study excited Ξ resonances.

II. STATUS OF THE GLUEX EXPERIMENT

In the following section, we discuss the current status of the development of the baseline GlueX experiment. The GlueX experiment was first presented to PAC 30 in 2006 [2]. While beam time was not awarded for 12 GeV proposals at that PAC, the proposal suggested a three phase startup for GlueX, which spanned approximately the first two calendar years of operation. Phase I covered detector commissioning. Phases II and III proposed a total of 7.5×10^6 s of detector live time at a flux of 10^7 γ/s for physics commissioning and initial exploratory searches for hybrid mesons. In 2010, an update of the experiment was presented to PAC 36 and a total of 120 days of beam time was granted for Phases I-III.

In 2008, two critical detector components were "descoped" from the design due to budgetary restrictions. First, and most importantly, the forward Cherenkov particle identification system was removed. The other component that was taken out was the level-three software trigger, which is needed for operating at a photon flux greater than 10^7 γ/s. These changes severely impact the ultimate scientific goals and discovery potential of the GlueX experiment, as was noted in the PAC report:

> Finally, the PAC would like to express its hope that the de-scoped Cherenkov detector be revisited at some time in the future. The loss of kaon identification from the current design is a real shame, but entirely understandable given the inescapable limitations on manpower, resources, and time.

We now propose the development of a kaon identification system to be used during a high intensity ($> 10^7$ γ/s) Phase IV running of GlueX. Such a system and beam intensity will allow systematic exploration of higher-mass $s\bar{s}$ states, with the goal of identifying $s\bar{s}$ members of the hybrid nonets and studying $s\bar{s}$ and $\ell\bar{\ell}$ $\left(|\ell\bar{\ell}\rangle \equiv (|u\bar{u}\rangle + |d\bar{d}\rangle)/\sqrt{2}\right)$ mixing amongst isoscalar mesons. A kaon identification system will also provide the capability needed to study doubly-strange Ξ baryons. In the remainder of this section, we review our progress toward the baseline GlueX construction, which is aimed at Phases I-III of running. Sections III and IV discuss the physics motivation for Phase IV, and Section V covers the Phase IV hardware and beam time requirements.

A. GlueX construction progress

A schematic view of the GlueX detector is shown in Fig. 3. All major components of the detector are under construction at Jefferson Lab or various collaborating institutions. Beam for the experiment is derived from coherent bremsstrahlung radiation from a thin diamond wafer and delivered to a liquid hydrogen target. The solenoidal detector has both central and forward tracking chambers as well as central and forward calorimeters. Timing and triggering are aided by a forward time of flight wall and a thin scintillator start counter that encloses the target. We briefly review the capabilities and construction status of each of the detector components below. The civil construction of Hall D is complete, and assembly of the detector within the hall is currently underway. Table I briefly lists all of the GlueX collaborating institutions and their primary responsibilities. The collaboration has grown significantly in the past four years; newer members are noted in the table.

1. *Beamline and Tagger*

The GlueX photon beam originates from coherent bremsstrahlung radiation produced by the 12 GeV electron beam impinging on a 20 μm diamond wafer. Orientation of the diamond and downstream collimation produces a photon beam peaked in energy around 9 GeV with about 40% linear polarization. A coarse tagger tags a broad range of electron energy, while precision tagging in the coherent peak is performed by a tagger microscope. A downstream pair spectrometer is utilized to measure photon conversions and determine the beam flux. Construction of the full system is underway.

Substantial work has also been done by the Connecticut group to fabricate and characterize thin diamond radiators for GlueX. This has included collaborations with the Cornell High Energy Synchrotron Source as well as industrial partners. Successful fabrication of 20 μm diamond radiators for GlueX seems possible. The design of the goniometer system to manipulate the diamond has

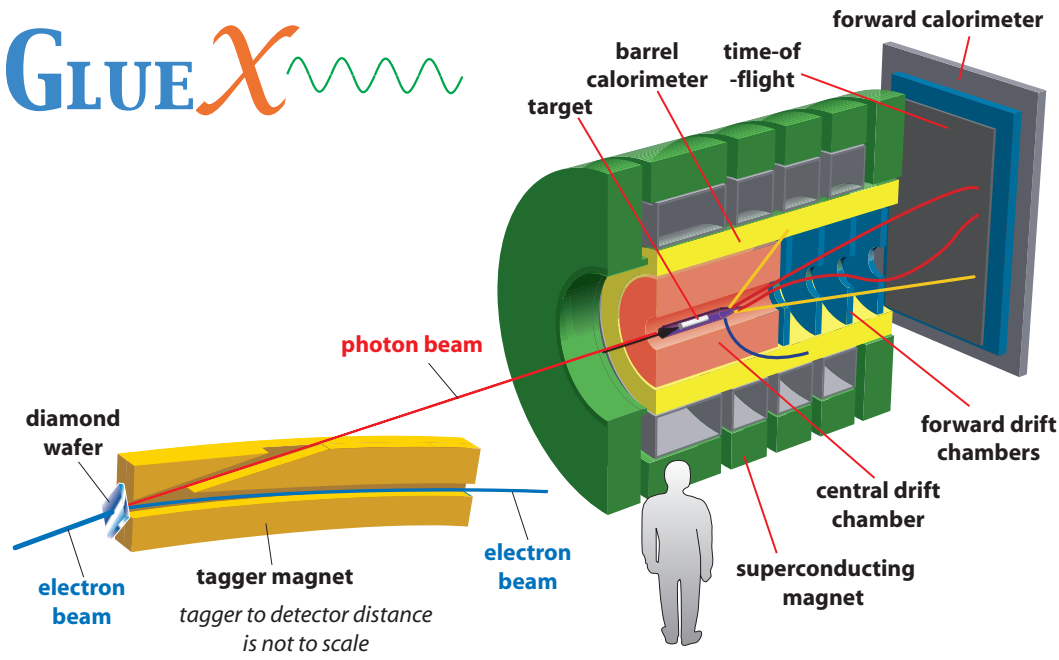

FIG. 3. A schematic of the GlueX detector and beam.

TABLE I. A summary of GlueX institutions and their responsibilities. The star (⋆) indicates that the group has joined GlueX after 2008.

Institution	Responsibilities
Arizona State U.⋆	beamline polarimetry, beamline support
Athens	BCAL and FCAL calibration
Carnegie Mellon U.	CDC, offline software, management
Catholic U. of America	tagger system
Christopher Newport U.	trigger system
U. of Connecticut	tagger microscope, diamond targets, offline software
Florida International U.	start counter
Florida State U.	TOF system, offline software
U. of Glasgow⋆	goniometer, beamline support
Indiana U.	FCAL, offline software, management
Jefferson Lab	FDC, data acquisition, electronics, infrastructure, management
U. of Massachusetts ⋆	target, electronics testing
Massachusetts Institute of Technology⋆	forward PID, offline software
MEPHI⋆	offline and online software
U. of North Carolina A&T State⋆	beamline support
U. of North Carolina, Wilmington⋆	pair spectrometer
U. Técnica Federico Santa María	BCAL readout
U. of Regina	BCAL, SiPM testing

been completed by the Glasgow group and is expected to be fabricated in 2012 by private industry.

The tagger magnet and vacuum vessel are currently being manufactured by industrial contractors, with winding of the coil starting in late April of 2012. These elements are expected to be installed in the tagger hall over the next eighteen months. The design for the precision tagger "microscope" has been developed at Connecticut, including the custom electronics for silicon photomultiplier (SiPM) readout. Beam tests of prototypes have been

conducted, and construction of the final system will begin in the fall of 2012. The coarse tagger, which covers the entire energy range up to nearly the endpoint, will be built by the Catholic University group. Work is underway to finalize the choice of photomultiplier tubes, and construction will start in the fall of 2012.

The groups from the University of North Carolina at Wilmington, North Carolina A&T State, and Jefferson Lab are collaborating to develop and construct the pair spectrometer. A magnet was obtained from Brookhaven and modified to make it suitable for use in Hall D. In addition, the Arizona State and Glasgow groups are collaborating to develop a technique for accurately measuring the linear polarization of the beam. Tests are planned in Mainz for the next year.

2. Solenoid

At the heart of the GlueX detector is the 2.2 T superconducting solenoid, which provides the essential magnetic field for tracking. The solenoidal geometry also has the benefit of reducing electromagnetic backgrounds in the detectors since low energy e^+e^- pairs spiral within a small radius of the beamline. The field is provided by four superconducting coils. Three of the four have been tested up to the nominal current of 1500 A – the remaining coil was only tested to 1200 A due to a problem with power leads that was unrelated to the coil itself. No serious problems have been found, and the magnet has now been fully assembled in Hall D. Both the cryogenic supply box and control systems will be developed this summer, and the plan is to start power tests of the assembled magnet in January.

Two years ago, there was great concern about the operational capabilities of the magnet, and the DOE required that we begin the process of building a replacement magnet. The conceptual design was subcontracted to MIT. The initial plan was to procure the technical design of the magnet with an option to build. However, given the recent successful tests of all the coils and the additional pressure to reduce overall project costs, development of the replacement solenoid has been halted and will likely be cancelled unless there are significant problems with the original magnet.

3. Tracking

Charged particle tracking is performed by two systems: a central straw-tube drift chamber (CDC) and four six-plane forward drift chamber (FDC) packages. The CDC is composed of 28 layers of 1.5 m-long straw tubes. The chamber provides $r-\phi$ measurements for charged tracks. Sixteen of the 28 layers have a 6° stereo angle to supply z measurements. Each FDC package is composed of six planes of anode wires. The cathode strips on either side of the anode cross at ±75° angles, providing a two-dimensional intersection point on each plane. Design and construction of the CDC [30] and FDC is ongoing at Carnegie Mellon University (CMU) and Jefferson Lab, respectively. The position resolution of the CDC and FDC is about 150 μm and 200 μm, respectively. Together the approximate momentum resolution is 2%, averaged over the kinematical regions of interest.

Construction on the CDC began in May of 2010 with initial procurement and quality assurance of components and the construction of a 400 ft^2 class 2000 cleanroom at CMU. In August, the end plates were mounted on the inner shell and then aligned. The empty frame was then moved into a vertical position for the installation of the 3522 straw tubes. This work started in November of 2010 and continued until October of 2011, when the outer shell was installed on the chamber. Stringing of the wires was completed in February of 2012, and all tension voltage and continuity checks were completed in March of 2012. In May of 2012, the upstream gas plenum will be installed on the chamber and the last labor-intensive phase started. This phase involves connecting each of the exposed crimp pins on the upstream end plate to the correct channel on a transition electronics board mounted on the end of the chamber. These boards have connectors that hold the high-voltage and preamplifier cards. The CDC will be delivered on time to Jefferson Lab in April of 2013 for installation into the GlueX detector.

After successful studies with a full-scale prototype, the FDC construction started in the beginning of 2011, with the entire production process carried out by Jefferson Lab in an off-site, 2000 ft^2 class 10,000 clean room. At the beginning of 2012, two months ahead of the schedule, two of the four packages had already been assembled. Tests of the first package have started with cosmic rays in a system that uses external chambers for tracking, scintillators for triggering, and a DAQ system. The package has exhibited very good HV stability; however, low chamber efficiency was traced to a problem with oxygen contamination. This problem was mitigated by redesigning the gas seal between the wire frames, and the revised design works as anticipated. The repair will need to be performed on the chambers that have already been fabricated; however, even with this delay, the production of all the FDC packages will be finished on schedule, by the end of this year.

4. Calorimetry

Like tracking, the GlueX calorimetry system consists of two detectors: a barrel calorimeter with a cylindrical geometry (BCAL) and a forward lead-glass calorimeter with a planar geometry (FCAL). The primary goal of these systems is to detect photons that can be used to reconstruct π^0's and η's, which are produced in the decays of heavier states. The BCAL is a relatively high-resolution sampling calorimeter, based on 1 mm double-clad Kuraray scintillating fibers embedded in a lead ma-

trix. It is composed of 48 4-m long modules; each module having a radial thickness of 15.1 radiation lengths. Modules are read out on each end by silicon SiPMs, which are not adversely affected by the high magnetic field in the proximity of the GlueX solenoid flux return. The forward calorimeter is composed of 2800 lead glass modules, stacked in a circular array. Each bar is coupled to a conventional phototube. The fractional energy resolution of the combined calorimetry system $\delta(E)/E$ is approximately 5%-6%/$\sqrt{E\ [\mathrm{GeV}]}$. Monitoring systems for both detectors have been designed by the group from the University of Athens.

All 48 BCAL calorimeter modules and a spare have been fabricated by the University of Regina and are currently in storage at Jefferson Lab, waiting to be fitted with light guides and sensors. A full module was tested extensively in Hall B in 2006 [31]; however, the readout for these tests used conventional phototubes instead of the final SiPMs. The production SiPMs are Hamamatsu S12045(X) MPPC arrays – currently about half of them have been delivered. Testing of the SiPMs is ongoing at Jefferson Lab and Universidad Técnica Federico Santa María (USM), with good consistency between each other and test data provided by Hamamatsu. The production light guides are being machined and polished at the USM. The first-article samples have been received and were used to instrument a final prototype, which is currently (in spring 2012) being tested with electrons in Hall B. Installation of the completed modules in the hall is expected to begin in the spring of 2013.

The 2800 lead glass modules needed for the FCAL have been assembled at Indiana University and shipped to Jefferson Lab. All of the PMTs will be powered by custom-built Cockroft-Walton style photomultiplier bases [32] in order to reduce cable mass, power dissipation, and high voltage control system costs. The design, fabrication, and testing of the bases is underway at Indiana University. All components for the FCAL will be delivered to Jefferson Lab for assembly to begin in the fall of 2012. A 25-block array utilizing the final design of all FCAL components was constructed and tested with electrons in Hall B in the spring of 2012; preliminary results indicate that the performance meets or exceeds expectations.

5. *Particle ID and timing*

The existing particle ID capabilities are derived from several subsystems. A dedicated forward time-of-flight wall (TOF), which is constructed from two planes of 2.5 cm-thick scintillator bars, provides about 70 ps timing resolution on forward-going tracks within about 10° of the beam axis. This information is complemented by time-of-flight data from the BCAL and specific ionization (dE/dx) measured with the CDC, both of which are particularly important for identifying the recoil proton in $\gamma p \to Xp$ reactions. Finally, identification of the beam bunch, which is critical for timing measurements, is performed by a thin start counter that surrounds the target.

For the TOF system, the type of plastic scintillator and photomultiplier tube has been chosen. We have built a prototype with these choices that achieves 100 ps resolution for mean time from a single counter read-out from both ends. The system consists of two planes of such counters, implying that the demonstrated two-plane resolution is 70 ps. The photomultiplier purchase is underway. The light guide design and material choice have been finalized. We are working on the design of the mechanical support and have a working concept. Soon we plan to build a full-scale mock-up of the central counters around the beam line to prove the mechanical design.

Engineering drawings for the start counter are under development. The counters and the electronics have to fit into a narrow space between the target vacuum chamber and the inner wall of the Central Drift Chamber. Prototypes have obtained time resolution of 300 to 600 ps, depending on the position of the hit along the length of the counter. The final segmentation has been fixed. SiPMs will be used for readout because they can be placed in the high magnetic field environment very close to the counters, thereby preserving scintillation light. The design of the SiPM electronics is about to start, and a final prototype of the scintillator assembly is under development.

The combined PID system in the baseline design is sufficient for identification of most protons in the kinematic regions of interest for GlueX. The forward PID can be used to enhance the purity of the charged pion sample. However, the combined momentum, path length, and timing resolution only allows for exclusive kaon identification for track momenta less than 2.0 GeV/c.

B. Initial physics goals and sensitivity

Phases I-III of the GlueX physics program provide an excellent opportunity for both the study of conventional mesons and the search for exotic mesons in photoproduction. Reconstructable final states will be limited to those decaying into non-strange states: π, η, η', and ω. Table II summarizes the expected lowest mass exotics and possible decay modes. Initial searches will likely focus on the π_1 isovector triplet and the η_1 isoscalar. It will also be important to try to establish the other (non-exotic) members of the hybrid multiplet: the 0^{-+}, 1^{--}, and 2^{-+} states. Finally, the initial data may provide an opportunity to search for the heavier exotic b_2 and h_2 states. Current lattice QCD predictions are that both the 1^{-+} (η_1 and η_1') and 2^{+-} (h_2 and h_2') isoscalars exhibit relatively little $\ell\bar{\ell} - s\bar{s}$ mixing (Fig. 1). It will be impossible to test this prediction or, if it is correct, to identify the η_1' and h_2' states without further kaon identification hardware.

One reaction of interest is $\gamma p \to \pi^+\pi^-\pi^+ n$. The $(3\pi)^{\pm}$ system has been studied extensively with data from E852 [33, 34], COMPASS [35], and CLAS [36], with COMPASS reporting evidence for exotic $\pi_1(1600) \to \rho\pi$

decay. In an attempt to exercise our software framework, a full analysis of mock GlueX data was performed with this channel. A GEANT-based simulation was developed to model all active and inactive material within the detector volume. Individual hits and background were simulated on all detector components, and reconstruction algorithms were utilized to reconstruct each event without knowledge of the true generated particles. Analysis of any final state depends on first exclusively selecting the reaction of interest and then performing an amplitude analysis to separate the various resonances that decay to that stable final state.

In order to test the detector capabilities for suppressing cross feed from other non-signal reactions, a PYTHIA-based generator was used to generate inclusive γp photoproduction at $E_\gamma = 9$ GeV. The signal events ($\gamma p \to \pi^+\pi^-\pi^+ n$) were generated at a level of about 2.5% of the total hadronic cross section. After optimizing all analysis criteria a signal selection efficiency of 25% and a signal-to-background ratio of 2:1 were achieved. About 20% of the total background originated from kaons misidentified as pions. The other backgrounds included protons being misidentified as pions or extra π^0's in the event that went undetected. This study, conducted in 2011, motivated a more detailed simulation of particle identification systems and tracking resolution along with enhancements in tracking efficiency. This work is still under development, and we expect that these enhanced algorithms along with improvements in analysis technique, such as kinematic fitting, will provide at least an order of magnitude further background suppression. Reducing the background to the percent level is essential for enhancing sensitivity in the amplitude analysis.

The sensitivity to small amplitudes that is provided by the GlueX detector acceptance and resolution was tested by performing an amplitude analysis on a sample of purely generated $\gamma p \to \pi^+\pi^-\pi^+ n$ events that has been subjected to full detector simulation and reconstruction as discussed above. Several conventional resonances, the a_1, π_2, and a_2, were generated along with a small ($< 2\%$) component of exotic π_1. The result of the fit is shown in Figure 4. This study indicates that with a pure sample of reconstructed decays, the GlueX detector provides excellent sensitivity to rare exotic decays. The analysis sensitivity will ultimately be limited by the ability to suppress and parametrize backgrounds in the amplitude analysis that arise from improperly reconstructed events, as noted above. While it is difficult to quantitatively predict the sensitivity with little knowledge of true detector performance or actual physics backgrounds, increased statistics and improved kaon identification will certainly lead to enhancements in sensitivity.

In order to take full advantage of GlueX statistics, high sample purity, which only comes with enhanced particle identification, is absolutely essential. For comparison, the 2008 run of COMPASS is expected to yield a final analyzable sample of order 10^8 events in the $\pi p \to 3\pi p$ channel [37], statistics comparable to the approved GlueX Phase II and III running. COMPASS will also have capability to positively identify kaons in the final state, enabling both high sample purity and the ability to explore $s\bar{s}$ states. While GlueX will utilize the complementary photoproduction mechanism, which has been argued to be rich in exotic production, it is important that both the statistical precision and sample purity remain competitive with state-of-the-art hadron beam experiments in order to maximize the collective and complementary physics output of all experiments.

III. STUDY OF $s\bar{s}$ MESONS

The primary goal of the GlueX experiment is to conduct a definitive mapping of states in the light meson sector with an emphasis on searching for exotic mesons. Ideally, we would like to produce the experimental analogue of the lattice QCD spectrum pictured in Fig. 1, enabling a direct test of our understanding of gluonic excitations in QCD. In order to achieve this, one must be able to reconstruct strange final states, as observing decay patterns of mesons has been one of the primary mechanisms of inferring quark flavor content. An example of this can be seen by examining the two lightest isoscalar 2^{++} mesons in the lattice QCD calculation in Fig. 1. The two states are nearly pure flavors with only a small (11°) mixing in the $\ell\bar{\ell}$ and $s\bar{s}$ basis. A natural experimental assignment for these two states are the $f_2(1270)$ and the $f_2'(1525)$. An experimental study of decay patterns shows that $\mathcal{B}(f_2(1270) \to KK)/\mathcal{B}(f_2(1270) \to \pi\pi) \approx 0.05$ and $\mathcal{B}(f_2'(1525) \to \pi\pi)/\mathcal{B}(f_2'(1525) \to KK) \approx 0.009$ [9], which support the prediction of an $f_2(1270)$ ($f_2'(1525)$) with a dominant $\ell\bar{\ell}$ ($s\bar{s}$) component. Without the ability to identify final state kaons, GlueX is incapable of providing similarly valuable experimental data to aid in the interpretation of the hybrid spectrum.

A. Exotic $s\bar{s}$ states

While most experimental efforts to date have focused on the lightest isovector exotic meson, the $J^{PC} = 1^{-+}$ $\pi_1(1600)$, lattice QCD clearly predicts a rich spectrum of both isovector and isoscalar exotics, the latter of which may have mixed $\ell\bar{\ell}$ and $s\bar{s}$ flavor content. A compilation of the "ground state" exotic hybrids is listed in Table II along with theoretical estimates for masses, widths, and key decay modes. It is expected that initial searches with the baseline GlueX hardware will be targeted primarily at the π_1 state. Searches for the η_1, h_0, and b_2 may be statistically challenging, depending on the masses of these states and the production cross sections. With increased statistics and kaon identification, the search scope can be broadened to include these heavier exotic states in addition to the $s\bar{s}$ states: η_1', h_0', and h_2'. The η_1' and h_2' are particularly interesting because some models predict these states to be relatively narrow and they should

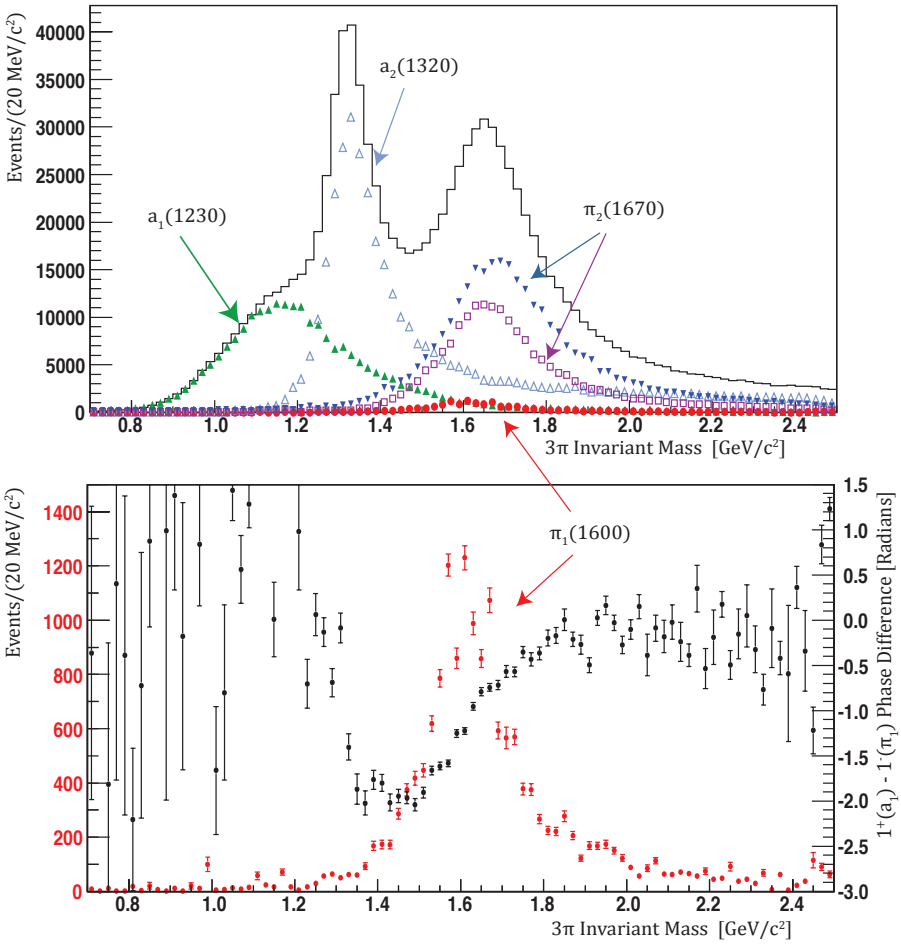

FIG. 4. A sample amplitude analysis result for the $\gamma p \to \pi^+\pi^-\pi^+ n$ channel with GlueX. (top) The invariant mass spectrum as a function of $M(\pi^+\pi^-\pi^+)$ is shown by the solid histogram. The results of the amplitude decomposition into resonant components in each bin is shown with points and error bars. (bottom) The exotic amplitude, generated at a relative strength of 1.6%, is cleanly extracted (red points). The black points show the phase between the π_1 and a_1 amplitudes.

decay through well-established kaon resonances.

The observation of various π_1 states has been reported in the literature for over fifteen years, with some analyses based on millions of events. However, it is safe to say that there exists a fair amount of skepticism regarding the assertion that unambiguous experimental evidence exists for exotic hybrid mesons. If the scope of exotic searches with GlueX is narrowed to only include the lightest isovector π_1 state, the ability for GlueX to comprehensively address the question of the existence of gluonic excitations in QCD is greatly diminished. On the other hand, clearly identifying all exotic members of the lightest hybrid multiplet, the three exotic $\pi_1^{\pm,0}$ states and the exotic η_1 and η_1', which can only be done by systematically studying a large number of strange and non-strange decay modes, would provide unambiguous experimental confirmation of exotic mesons. A study of decays to kaon final states could demonstrate that the η_1 candidate is dominantly $\ell\bar{\ell}$ while the η_1' candidate is $s\bar{s}$, as predicted by initial lattice QCD calculations. Such a discovery would represent a substantial improvement in the experimental understanding of exotics – an improvement that cannot be made by simply collecting more data with the baseline GlueX detector configuration. In addition, further identification of members of the 0^{+-} and 2^{+-} nonets as well as measuring the mass splittings with the 1^{+-} states will validate the phenomenological picture that is emerging from lattice QCD of these states as P-wave couplings of a gluonic field with a color-octet $q\bar{q}$ system.

TABLE II. A compilation of exotic quantum number hybrid approximate masses, widths, and decay predictions. Masses are estimated from dynamical LQCD calculations with $M_\pi = 396$ MeV/c^2 [1]. The PSS (Page, Swanson and Szczepaniak) and IKP (Isgur, Kokoski and Paton) model widths are from Ref. [38], with the IKP calculation based on the model in Ref. [39]. The total widths have a mass dependence, and Ref. [38] uses somewhat different mass values than suggested by the most recent lattice calculations [1]. Those final states marked with a dagger (†) are ideal for experimental exploration because there are relatively few stable particles in the final state or moderately narrow intermediate resonances that may reduce combinatoric background. (We consider η, η', and ω to be stable final state particles.)

	Approximate Mass (MeV)	J^{PC}	Total Width (MeV) PSS	IKP	Relevant Decays	Final States
π_1	1900	1^{-+}	80 – 170	120	$b_1\pi^\dagger$, $\rho\pi^\dagger$, $f_1\pi^\dagger$, $a_1\eta$, $\eta'\pi^\dagger$	$\omega\pi\pi^\dagger$, $3\pi^\dagger$, 5π, $\eta 3\pi^\dagger$, $\eta'\pi^\dagger$
η_1	2100	1^{-+}	60 – 160	110	$a_1\pi$, $f_1\eta^\dagger$, $\pi(1300)\pi$	4π, $\eta 4\pi$, $\eta\eta\pi\pi^\dagger$
η_1'	2300	1^{-+}	100 – 220	170	$K_1(1400)K^\dagger$, $K_1(1270)K^\dagger$, $K^*K^\dagger$	$KK\pi\pi^\dagger$, $KK\pi^\dagger$, $KK\omega^\dagger$
b_0	2400	0^{+-}	250 – 430	670	$\pi(1300)\pi$, $h_1\pi$	4π
h_0	2400	0^{+-}	60 – 260	90	$b_1\pi^\dagger$, $h_1\eta$, $K(1460)K$	$\omega\pi\pi^\dagger$, $\eta 3\pi$, $KK\pi\pi$
h_0'	2500	0^{+-}	260 – 490	430	$K(1460)K$, $K_1(1270)K^\dagger$, $h_1\eta$	$KK\pi\pi^\dagger$, $\eta 3\pi$
b_2	2500	2^{+-}	10	250	$a_2\pi^\dagger$, $a_1\pi$, $h_1\pi$	4π, $\eta\pi\pi^\dagger$
h_2	2500	2^{+-}	10	170	$b_1\pi^\dagger$, $\rho\pi^\dagger$	$\omega\pi\pi^\dagger$, $3\pi^\dagger$
h_2'	2600	2^{+-}	10 – 20	80	$K_1(1400)K^\dagger$, $K_1(1270)K^\dagger$, $K_2^*K^\dagger$	$KK\pi\pi^\dagger$, $KK\pi^\dagger$

B. Non-exotic $s\bar{s}$ mesons

As discussed in Section I A, one expects the lowest-mass hybrid multiplet to contain $(0,1,2)^{-+}$ states and a 1^{--} state that all have about the same mass and correspond to an S-wave $q\bar{q}$ pair coupling to the gluonic field in a P-wave. For each J^{PC} then we expect an isovector triplet and a pair of isoscalar states in the spectrum. Of the four sets of J^{PC} values for the lightest hybrids, only the 1^{-+} is exotic. The other hybrid states will appear as supernumerary states in the spectrum of conventional mesons. The ability to clearly identify these states depends on having a thorough and complete understanding of the meson spectrum. Like searching for exotics, a complete mapping of the spectrum of non-exotic mesons requires the ability to systematically study many strange and non-strange final states. Other experiments, such as BESIII, are carefully studying this region utilizing of order 10^9 hadronic decays of charmonium and have outstanding capability to cleanly study any possible final state. While the production mechanism of GlueX is complementary to that of charmonium decay and is thought to enhance hybrid production, it is essential that the detector capability and statistical precision of the data set be competitive with other contemporary experiments in order to maximize the collective experimental knowledge of the meson spectrum. Hybrid mesons with non-exotic J^{PC} are also expected to appear in the spectrum in the proximity of the exotic $(0,2)^{+-}$ states.

Given the recent developments in charmonium (briefly discussed in Section I B), a state that has attracted a lot of attention in the $s\bar{s}$ spectrum is the $Y(2175)$, which is assumed to be an $s\bar{s}$ vector meson (1^{--}). The $Y(2175)$ has been observed to decay to $\pi\pi\phi$ and has been produced in both J/ψ decay [26] and e^+e^- collisions [25, 27]. The state is a proposed analogue of the $Y(4260)$ in charmonium, a state that is also about 1.2 GeV heavier than the ground state triplet (J/ψ) and has a similar decay mode: $Y(4260) \to \pi\pi J/\psi$. The $Y(4260)$ has no obvious interpretation in the charmonium spectrum and has been speculated to be a hybrid meson [40–43], which, by loose analogy, leads to the implication that the $Y(2175)$ might also be a hybrid candidate. It should be noted that the spectrum of 1^{--} $s\bar{s}$ mesons is not as well-defined experimentally as the $c\bar{c}$ system; therefore, it is not clear that the $Y(2175)$ is a supernumerary state. However, GlueX is ideally suited to study this system. We know that vector mesons are copiously produced in photoproduction; therefore, with the ability to identify kaons, a precision study of the 1^{--} $s\bar{s}$ spectrum can be conducted with GlueX. Some have predicted [44] that the potential hybrid nature of the $Y(2175)$ can be explored by studying ratios of branching fractions into various kaonic final states. In addition, should GlueX be able to conclude that the $Y(2175)$ is in fact a supernumerary vector meson, then a search can be made for the exotic 1^{-+} $s\bar{s}$ member of the multiplet (η_1'), evidence of which would provide a definitive interpretation of the $Y(2175)$ and likely have implications on how one interprets charmonium data.

IV. Ξ BARYONS

The spectrum of multi-strange hyperons is poorly known, with only a few well-established resonances. Among the doubly-strange states, the two ground-state Cascades, the octet member $\Xi(1320)$ and the decuplet member $\Xi(1530)$, have four-star status in the PDG [9], with only four other three-star candidates. On the other hand, more than 20 N^* and Δ^* resonances are rated

with at least three stars in the PDG. Of the six Ξ states that have at least three-star ratings in the PDG, only two are listed with weak experimental evidence for their spin-parity (J^P) quantum numbers: $\Xi(1530)\frac{3}{2}^+$ [45], $\Xi(1820)\frac{3}{2}^-$ [46]. All other J^P assignments are based on quark-model predictions. Flavor $SU(3)$ symmetry predicts as many Ξ resonances as N^* and Δ^* states combined, suggesting that many more Cascade resonances remain undiscovered. The three lightest quarks, u, d, and s, have 27 possible flavor combinations: $3 \otimes 3 \otimes 3 = 1 \oplus 8 \oplus 8' \oplus 10$ and each multiplet is identified by its spin and parity, J^P. Flavor $SU(3)$ symmetry implies that the members of the multiplets differ only in their quark makeup, and that the basic properties of the baryons should be similar, although the symmetry is known to be broken by the strange-light quark mass difference. The octets consist of N^*, Λ^*, Σ^*, and Ξ^* states. We thus expect that for every N^* state, there should be a corresponding Ξ^* state *with similar properties*. Additionally, since the decuplets consist of Δ^*, Σ^*, Ξ^*, and Ω^* states, we also expect for every Δ^* state to find a decuplet Ξ^* with similar properties.

A. Ξ spectrum and decays

The Ξ hyperons have the unique feature of double strangeness: $|ssu\rangle$ and $|ssd\rangle$. If the confining potential is independent of quark flavor, the energy of spatial excitations of a given pair of quarks is inversely proportional to their reduced mass. This means that the lightest excitations in each partial wave are between the two strange quarks. In a spectator decay model, such states will not decay to the ground state Ξ and a pion because of orthogonality of the spatial wave functions of the two strange quarks in the excited state and the ground state. This removes the decay channel with the largest phase space for the lightest states in each partial wave, substantially reducing their widths. Typically, Γ_{Ξ^*} is about $10-20$ MeV for the known lower-mass resonances, which is $5-30$ times narrower than for N^*, Δ^*, Λ^*, and Σ^* states. These features, combined with their isospin of 1/2, render possible a wide-ranging program on the physics of the Cascade hyperon and its excited states. Until recently, the study of these hyperons has centered on their production in K^-p reactions; some Ξ^* states were found using high-energy hyperon beams. Photoproduction appears to be a very promising alternative. Results from earlier kaon beam experiments indicate that it is possible to produce the Ξ ground state through the decay of high-mass Y^* states [47–49]. It is therefore possible to produce Cascade resonances through t-channel photoproduction of hyperon resonances using the photoproduction reaction $\gamma p \to KK\Xi^{(*)}$ [28, 29].

In briefly summarizing a physics program on Cascades, it would be interesting to see the lightest excited Ξ^* states in certain partial waves decoupling from the $\Xi\pi$ channel, confirming the flavor independence of confinement. Measurements of the isospin splittings in spatially excited Cascade states are also possible for the first time in a spatially excited hadron. Currently, these splittings like $n-p$ or $\Delta^0-\Delta^{++}$ are only available for the octet and decuplet ground states, but are hard to measure in excited N, Δ and Σ, Σ^* states, which are very broad. The lightest Cascade baryons are expected to be narrower, and measuring the $\Xi^- - \Xi^0$ splitting of spatially excited Ξ states remains a strong possibility. These measurements are an interesting probe of excited hadron structure and would provide important input for quark models, which describe the isospin splittings by the u- and d-quark mass difference as well as by the electromagnetic interactions between the quarks.

B. Ξ searches using the GlueX experiment

The Cascade octet ground states (Ξ^0, Ξ^-) can be studied in the GlueX experiment via exclusive t-channel (meson exchange) processes in the reactions:

$$\begin{aligned}\gamma p \;\to\; K\,Y^* \;\to\; & K^+\,(\,\Xi^-\,K^+\,),\\ & K^+\,(\,\Xi^0\,K^0\,),\\ & K^0\,(\,\Xi^0\,K^+\,).\end{aligned} \tag{1}$$

The production of such two-body systems involving a Ξ particle also allows for studying high-mass Λ^* and Σ^* states. The Cascade decuplet ground state, $\Xi(1530)$, and other excited Cascades decaying to $\Xi\pi$ can be searched for and studied in the reactions:

$$\begin{aligned}\gamma p \;\to\; K\,Y^* \;\to\; & K^+\,(\,\Xi\,\pi\,)\,K^0,\\ & K^+\,(\,\Xi\,\pi\,)\,K^+,\\ & K^0\,(\,\Xi\,\pi\,)\,K^+.\end{aligned} \tag{2}$$

The lightest excited Ξ states are expected to decouple from $\Xi\pi$ and can be searched for and studied in their decays to $\Lambda\bar{K}$ and $\Sigma\bar{K}$:

$$\begin{aligned}\gamma p \;\to\; K\,Y^* \;\to\; & K^+\,(\,\bar{K}\Lambda\,)_{\Xi^{-*}}\,K^+,\\ & K^+\,(\,\bar{K}\Lambda\,)_{\Xi^{0*}}\,K^0,\\ & K^0\,(\,\bar{K}\Lambda\,)_{\Xi^{0*}}\,K^+,\end{aligned} \tag{3}$$

$$\begin{aligned}\gamma p \;\to\; K\,Y^* \;\to\; & K^+\,(\,\bar{K}\Sigma\,)_{\Xi^{-*}}\,K^+,\\ & K^+\,(\,\bar{K}\Sigma\,)_{\Xi^{0*}}\,K^0,\\ & K^0\,(\,\bar{K}\Sigma\,)_{\Xi^{0*}}\,K^+.\end{aligned} \tag{4}$$

Backgrounds from competing hadronic reactions will be reducible because of the unique signature provided by the two associated kaons in Ξ photoproduction in combination with secondary vertices, stemming from weak decays of ground-state hyperons. However, decays such as $Y^* \to \phi\Lambda$, $\phi\Sigma$ might contribute for certain final states. Larger contributions to the background will more likely come from events with pions misidentified as kaons as well as other reconstruction and detector inefficiencies. To extract small Cascade signals at masses above the $\Xi(1530)$, it will therefore be important to reduce the

background by reconstructing kinematically complete final states that include kaons. A full exclusive reconstruction also enhances the possibility of being able to measure the J^P of these states.

V. GLUEX HARDWARE AND BEAM TIME REQUIREMENTS

In order to maximize the discovery capability of GlueX, an enhanced capability to identify kaons coupled with an increase in statistical precision is needed. In this section, we detail those needs as well as provide two possible conceptual designs for a kaon detector. To maximize sensitivity, we propose a gradual increase in the photon flux towards the GlueX design of 10^8 γ/s in the peak of the coherent bremsstrahlung spectrum (8.4 GeV $< E_\gamma <$ 9.0 GeV). Yield estimates, assuming an average flux of 5×10^7 γ/s, are presented. In order to minimize the bandwidth to disk and ultimately enhance analysis efficiency, we propose the addition of a level-three software trigger to the GlueX data acquisition system. We should note that the GlueX detectors and data acquisition architecture are designed to handle a rate of 10^8 γ/s. However, the optimum photon flux for taking data will depend on the event reconstruction at high luminosity and needs to be studied under realistic experimental conditions. If our extraction of amplitudes is not statistics limited, we may optimize the flux to reduce systematic errors.

A. Kaon identification in GlueX

In order to understand how decays of heavy exotic $s\bar{s}$ mesons might populate the GlueX detector, we simulated several channels noted in Table II. Each was simulated with a production cross section proportional to $e^{-5|t|}$, where $|t|$ is the four-momentum transfer squared from the photon to the nucleon[2]. Figure 5 shows how four key reactions populate the space of kaon momentum and polar angle. Assuming a momentum resolution of 2%, a path length resolution of 3 cm, and a timing resolution of 70 ps, the existing forward TOF detector provides four standard deviations of separation between kaons and pions in the region of $1^\circ - 10^\circ$ and < 2.0 GeV/c (indicated by the red box in Figs. 5). One can see that the system is clearly inadequate for efficiently detecting kaons produced in these key reactions.

We have also simulated the production of the $\Xi^-(1320)$ and $\Xi^-(1820)$ resonances to better understand the kinematics of these reactions. The photoproduction of the $\Xi^-(1320)$ decaying to $\pi^-\Lambda$ and of the $\Xi^-(1820)$ decaying to ΛK^- are shown in Fig. 6. These reactions result in $K^+K^+\pi^-\pi^-p$ and $K^+K^+K^-\pi^-p$ final states, respectively. Reactions involving excited Cascades have "softer" forward-going kaons, and there is more energy available on average to the Cascade's decay products. Both plots show three regions of high density. The upper momentum regions (> 4 GeV/c) consist of forward-going K^+ tracks from the associated production of an excited hyperon. The middle momentum regions (0.6-2.0 GeV/c) are a mixture of kaon and proton tracks, while the lower regions (< 0.6 GeV/c) contain mostly π^- tracks. The kaon tracks with momenta larger than about 2.0 GeV/c cannot be positively identified with the current GlueX PID system. Accurate particle identification will be essential for rejection of background events. The addition of a forward kaon identification system will allow for the separation of fast, forward-going kaons from pions, cleaning up the event sample.

Two types of Cherenkov detectors that are commonly used for particle identification are the threshold Cherenkov detector and the ring-imaging Cherenkov (RICH) detector. In a threshold Cherenkov detector, a radiator is chosen such that, at a fixed momentum, pions emit Cherenkov radiation, but heavier kaons do not. The kaon identification is therefore performed by assuming that charged tracks that are not pions are kaons. The goal of a RICH is to image the Cherenkov cone emitted by all charged particles traversing the radiator. By using a thin radiator, the emitted Cherenkov light projects an elliptical ring onto the detector. The measured Cherenkov angle along with the momentum can be used to infer the particle mass. The RICH is capable of positively identifying all three common species of hadrons: pions, kaons, and protons.

Below we discuss conceptual designs for both types of detectors. Neither of the two designs presented are final – the GlueX Collaboration is actively working on design and simulation of detectors in order to develop a forward particle identification solution that is optimized for the GlueX physics program.

1. *Threshold gas Cherenkov*

The initial GlueX proposal included the construction of a threshold gas Cherenkov detector in between the solenoid and the forward time-of-flight systems. A single C_4F_{10} gas radiator with an index of refraction $n = 1.0015$ was proposed, which has a pion momentum threshold for Cherenkov radiation at 2.5 GeV/c. The design utilized two sets of focussing mirrors to reflect the light into phototubes. A conceptual drawing along with proposed placement in the GlueX detector is shown in Fig. 7. If the threshold for detection is set at about five photoelectrons, then the proposed detector would be capable of providing a pion veto above 3 GeV/c momentum in the region less than 10°. This detector would greatly

[2] For t production coefficients less (greater) than 5 GeV^{-2}, we expect the acceptance to increase (decrease). The true t dependence is unknown for the reaction of interest; therefore, we use 5 GeV^{-2} as a conservative estimate.

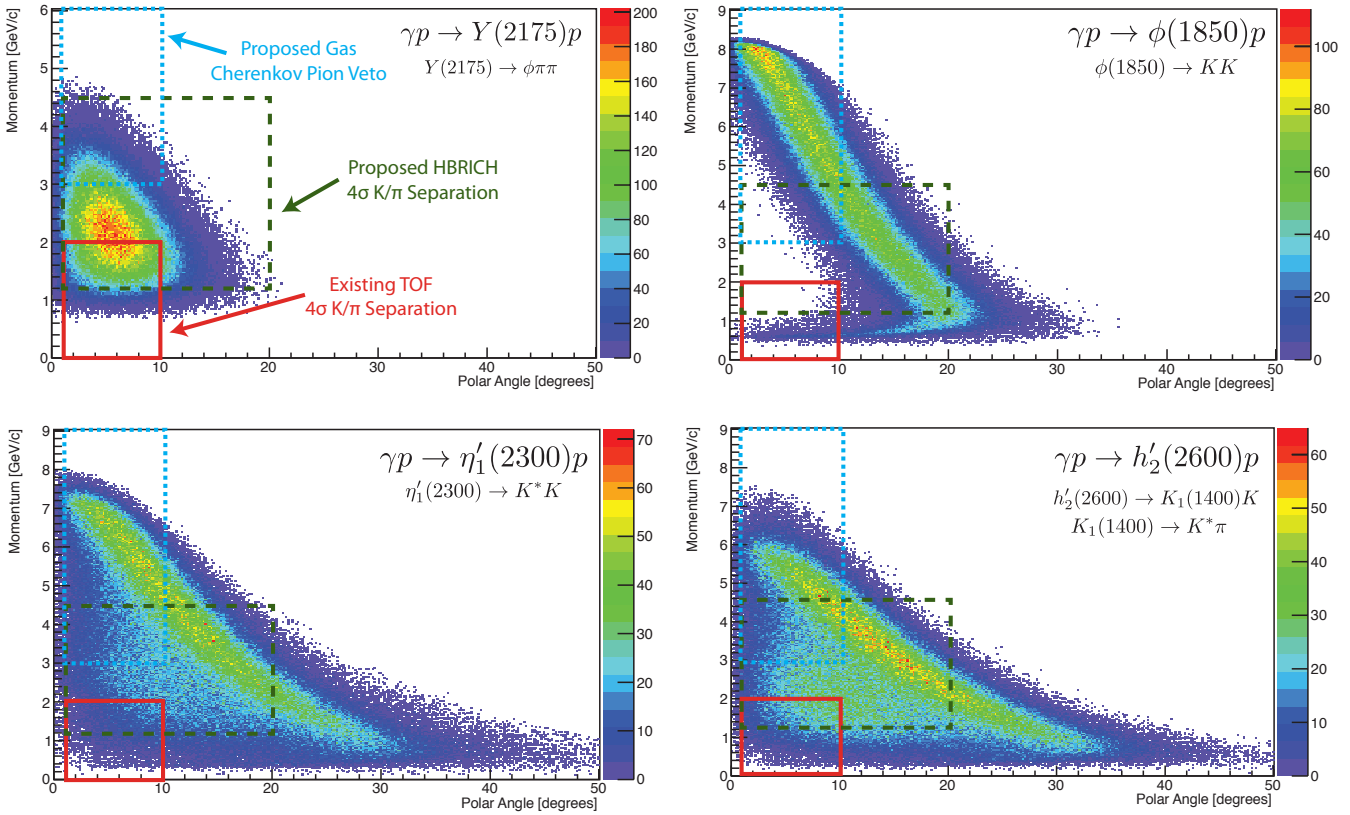

FIG. 5. Plots of particle density as a function of momentum and polar angle for all kaons in a variety of different production channels. Shown in solid (red), dashed (green), and dotted (blue) are the regions of phase space where the existing time-of-flight (TOF) detector, proposed HBRICH, and proposed gas Cherenkov provide pion/kaon discrimination at the four standard deviation level.

improve the kaon detection efficiency over the time-of-flight system; however, detection would still be limited to the forward direction, and a gap in detection capability exists for kaon momenta between 2.0 and 3.0 GeV/c. In addition, no separation between kaons and protons is provided, as neither will generate Cherenkov radiation in C_4F_{10} in the momentum range of interest. (Kaons begin to radiate around 9 GeV/c.) A secondary radiator, *e.g.* aerogel, may enhance the performance. A final concern is the background rate in the detector. We know that the dominant background is e^+e^- pairs generated by interactions of the photon beam with material. Detectors near the GlueX beamline, *e.g.,* the FCAL, FDC, and TOF, are expected to experience electromagnetic background at the MHz level. Significant backgrounds may lead to false rejection of true kaons. For comparison, the region of kaon phase space where the threshold gas Cherenkov detector would effectively operate as a pion veto is indicated in Figs. 5 and 6 with a blue dotted line.

2. *Hadron blind RICH*

With the goal of having positive kaon identification up to momenta of 4.5 GeV/c and enhancing the angular coverage up to 20°, a conceptual design for a "hadron blind RICH" (HBRICH) detector for GlueX has been developed. The detector is inspired by the existing proximity focusing RICH detector in use in Hall A, which utilizes CsI to convert the Cherenkov photons to electrons [50]. In order to make the detector blind to ionization produced by hadrons traversing the expansion volume, a reverse bias is applied to clear the volume of ionization electrons. Such a technique was pioneered by the PHENIX hadron blind detector [51]. A sketch of the detector, along with its proposed placement, is shown in Fig. 7. The upstream end cap contains the primary radiator, followed by a mesh electrode to provide reverse bias. The barrel of the detector (1.9 m^2) and the downstream end cap (1.1 m^2) will be covered by three-stage gas electron multiplier (GEM) foils [52] together with pad readout that records the image charge of the electron avalanche on the GEM. The center volume can be filled with gas as the secondary radiator to provide complementary PID

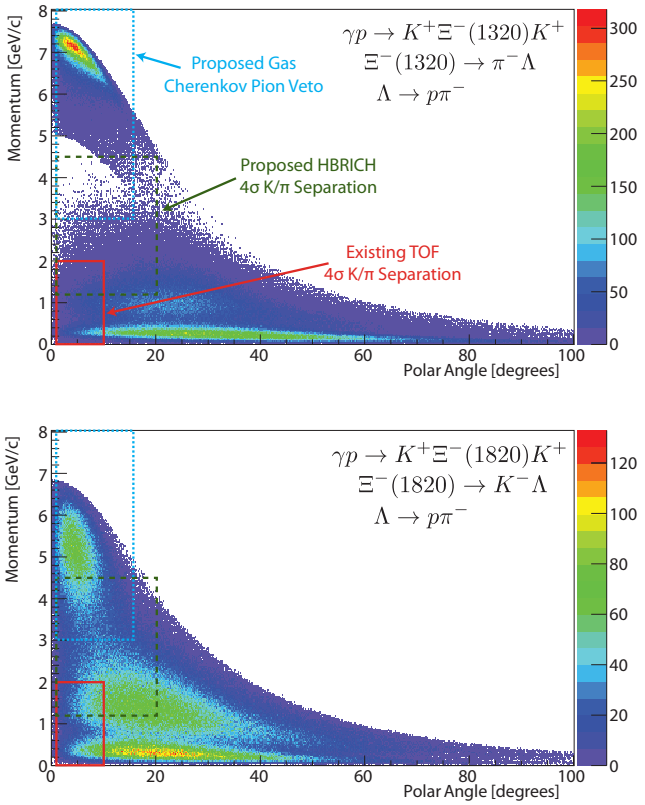

FIG. 6. Generated momentum versus polar angle for all tracks in the simulated reactions (top) $\gamma p \to K^+\,\Xi^-(1320)K^+$ and (bottom) $\gamma p \to K^+\,\Xi^-(1820)K^+$. The three high-density regions in each plot are populated with, from lowest to highest momentum, pions, kaons and protons, and kaons. Regions of coverage for various particle identification detectors are indicated.

capability and enhance the range of momenta covered by the detector.

We can make a rough estimate of the number of readout channels needed for the design described above. An $n = 1.1$ radiator, *e.g.*, aerogel, provides angular separation of kaons and pions within the momentum range of interest. At 4.5 GeV/c, the Cherenkov angles of kaons and pions differ by about 14 mrad after photons are refracted from the radiator into the detector volume. Assuming an average of 10 photoelectrons per track, in order to reach a 4σ separation, the maximum size for the readout pads is about 19 mm. A 15 mm $\times$ 15 mm pad is sufficient for the end cap. The barrel readout may need double the resolution in one direction to accommodate the elliptical projection of the rings. The total number of channels would be approximately 22,000, which is of a comparable scale to the number of channels in the GlueX FDC. The projected momentum and angular coverage of the HBRICH is shown in Figs. 5 and 6 with a green dashed line.

In comparison to the gas threshold Cherenkov, the design and development of an HBRICH is notably more challenging. While portions of the design are inspired by existing detectors, a detector like the HBRICH has never been constructed. The detector would require the insertion of a large amount of material into the active tracking volume, which could have adverse effects on tracking resolution and calorimeter efficiency. While there is a lot of activity in the development of large-area GEM foils [53] driven by the desire to build high-resolution time projection chambers, GEM-based detectors of the scale of the proposed HBRICH have not yet been constructed. In addition, significant work is needed to develop a large scale GEM readout for such a detector. The gas threshold Cherenkov, on the other hand, is based primarily of proven technology that has been used in many detectors for decades. Either detector would provide a significant enhancement in the kaon identification capability of GlueX and greatly expand the discovery potential of the experiment.

The collaboration is also exploring other options. For example, a dual radiator (aerogel and C_4F_{10}) RICH, similar to that developed for LHCb [54], could fit in the region of the proposed threshold gas Cherenkov detector. Assuming the same performance demonstrated by LHCb is achievable in GlueX, this detector would provide positive kaon and pion identification for particles with momenta greater than 1 GeV/c; however, its angular coverage would be limited to the region $< 10^\circ$ about the beam axis. As noted above, the collaboration has an active program of detector design ongoing and is expected to reach a final design decision within the next six months.

B. Desired beam time and intensity

One can estimate the total number of observed events in some stable final state N_i using the following equation.

$$N_i = \epsilon_i \sigma_i n_\gamma n_t T, \tag{5}$$

where ϵ_i and σ_i are the detection efficiency and photoproduction cross section of the final state i, n_γ is the rate of incident photons on target, n_t is the number of scattering centers per unit area, and T is the integrated live time of the detector. For a 30 cm LH_2 target, n_t is 1.26 b^{-1}. (A useful rule of thumb is that at $n_\gamma = 10^7$ γ/s a 1 μb cross section will result in the production of about 10^6 events per day.) It is difficult to estimate the production cross section for many final states since data in the GlueX energy regime are sparse. (For a compendium of photoproduction cross sections, see Ref. [55].) Table III lists key final states for initial exotic hybrid searches along with assumed production cross sections[3].

[3] Some estimates are based on actual data from Ref. [55] for cross sections at a similar beam energy, while others are crudely es-

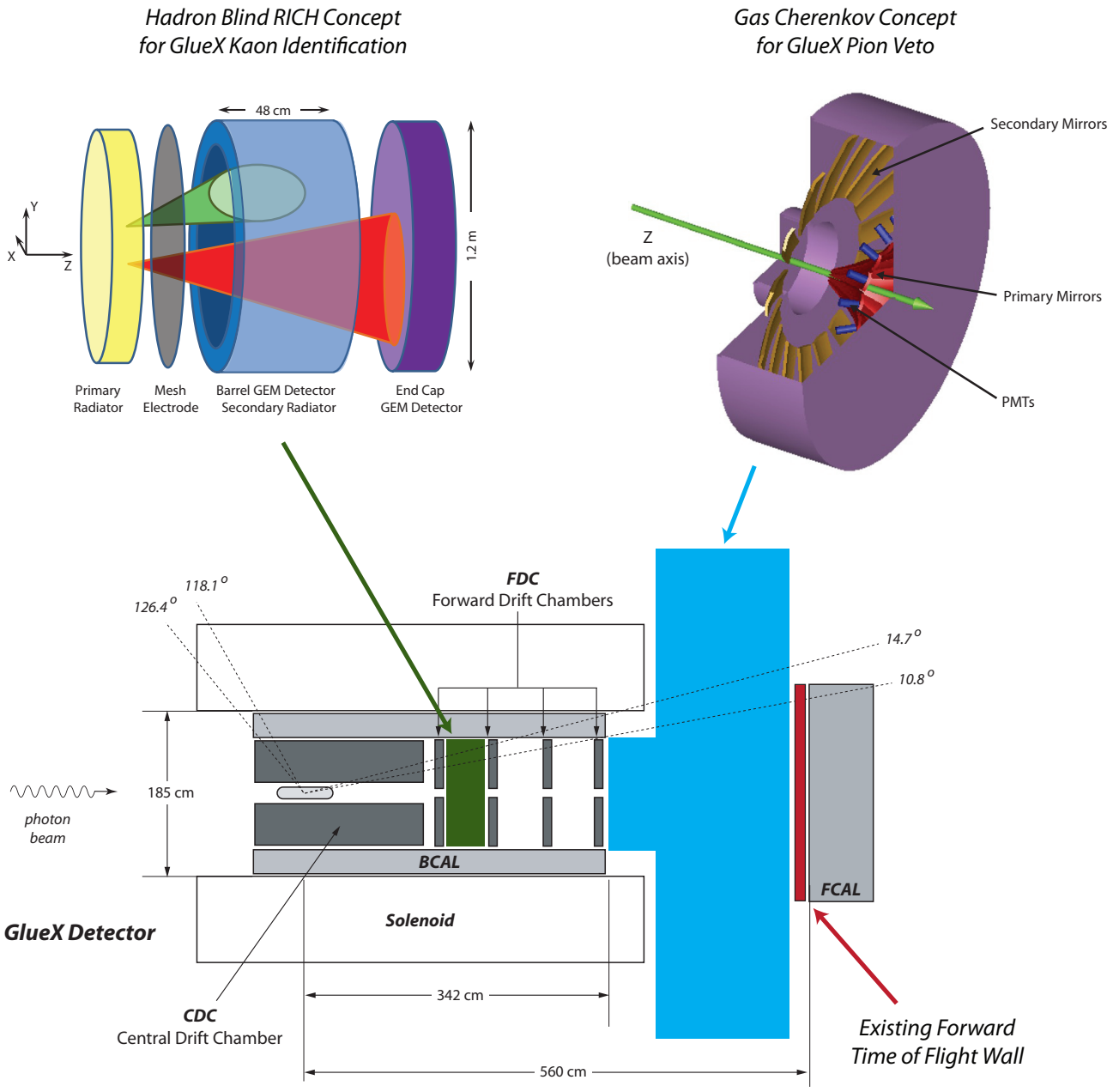

FIG. 7. Conceptual drawings of both the hadron blind RICH (HBRICH) and threshold gas Cherenkov detectors and their proposed locations within the GLUEX detector.

In order to estimate the total yield in Phase II and III running, we assume 90 PAC days of beam[4] and estimate that 80% of the delivered beam will be usable for analysis (about 6×10^6 s total) at an intensity of $n_\gamma = 10^7$ γ/s in the coherent bremsstrahlung peak. For the proposed Phase IV running, we assume 200 PAC days of beam with 80% usable for physics analysis and an *average intensity* of 5×10^7 γ/s. We assume the detection efficiency for protons, pions, kaons, and photons to be 70%, 80%, 70%, and 80%, respectively. Of course, the true efficiencies are dependent on software algorithms, kinematics, multiplicity, and other variables; however, the dominant uncertainty in yield estimates is not efficiency but cross section.

timated from the product of branching ratios of heavy meson decays, *i.e.,* a proxy for light meson hadronization ratios, and known photoproduction cross sections.

[4] We plan to utilize 30 of the 120 approved PAC days for the Phase I commissioning of the detector.

TABLE III. A table of hybrid search channels, estimated cross sections, and approximate numbers of observed events. See text for a discussion of the underlying assumptions. The subscripts on ω, η, and η' indicate the decay modes used in the efficiency calculations. If explicit charges are not indicated, the yields represent an average over various charge combinations.

Final State	Cross Section (μb)	Approved Phase II and III ($\times 10^6$ events)	*Proposed* Phase IV ($\times 10^6$ events)
$\pi^+\pi^-\pi^+$	10	300	3000
$\pi^+\pi^-\pi^0$	2	50	600
$KK\pi\pi$	0.5	–	100
$\omega_{3\pi}\pi\pi$	0.2	4	40
$\omega_{\gamma\pi}\pi\pi$	0.2	0.6	6
$\eta_{\gamma\gamma}\pi\pi$	0.2	3	30
$\eta_{\gamma\gamma}\pi\pi\pi$	0.2	2	20
$\eta'_{\gamma\gamma}\pi$	0.1	0.1	1
$\eta'_{\eta\pi\pi}\pi$	0.1	0.3	3
$KK\pi$	0.1	–	30

These assumed efficiencies reproduce signal selection efficiencies in detailed simulations of $\gamma p \to \pi^+\pi^-\pi^+ n$, $\gamma p \to \eta\pi^0 p$, $\gamma p \to b_1^{\pm}\pi^{\mp} p$, and $\gamma p \to f_1\pi^0 p$ performed by the collaboration.

Photoproduction of mesons at 9 GeV proceeds via peripheral production (sketched in the inset of Fig. 8). The production can typically be characterized as a function of $t \equiv (p_X - p_\gamma)^2$, with the production cross section proportional to $e^{-\alpha|t|}$. The value of α for measured reactions ranges from 3 to 10 GeV^{-2}. This t-dependence, which is unknown for many key GlueX reactions, results in a suppression of the rate at large values of $|t|$, which, in turn, suppresses the production of high mass mesons. Figure 8 shows the minimum value of $|t|$ as a function of the produced meson mass M_X for a variety of different photon energies. The impact of this kinematic suppression on a search for heavy states is illustrated in Figure 9, where events are generated according to the t distributions with both $\alpha = 5$ GeV^{-2} and 10 GeV^{-2} and uniform in M_X. Those that are kinematically allowed ($|t| > |t|_{\rm min}$) are retained. The y-axis indicates the number of events in 10 MeV/c^2 mass bins, integrated over the allowed region in t, and assuming a total of 3×10^7 events are collected. The region above $M_X = 2.5$ GeV/c^2, where one would want to search for states such as the h_2 and h'_2, contains only about 5% of all events due to the suppression of large $|t|$ that is characteristic of peripheral photoproduction.

There are several considerations in determining how much data one needs in any particular final state. In order to perform an amplitude analysis of the final state particles, one typically separates the data into bins of momentum transfer t and resonance mass M_X. The number of bins in t could range from one to greater than ten, depending on the statistical precision of the data; a study of the t-dependence, if statistically permitted, provides valuable information on the production dynamics of particular resonances. One would like to make the mass bins as small as possible in order to maximize sensitivity to states that have a small total decay width; however, it is not practical to use a bin size that is smaller than the resolution on M_X, which is of order 10 MeV/c^2. In each bin of t and M_X, one then needs enough events to perform an amplitude analysis, which is about 10^4. Figure 9 demonstrates that, under some assumptions about the production, this level of statistics is achievable for

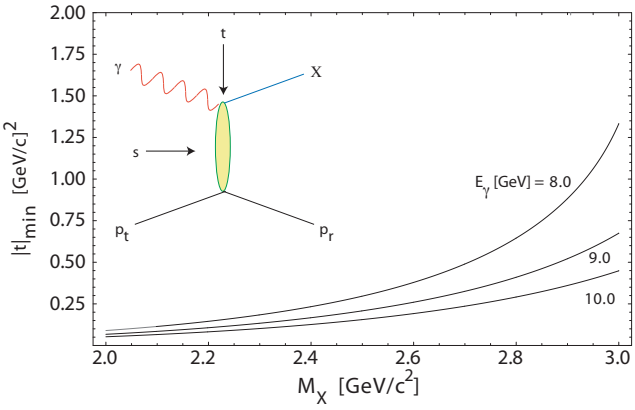

FIG. 8. Dependence of $|t|_{\rm min}$ on the mass of the outgoing meson system M_X. The lines indicate incident photon energies of 8.0, 9.0, and 10.0 GeV.

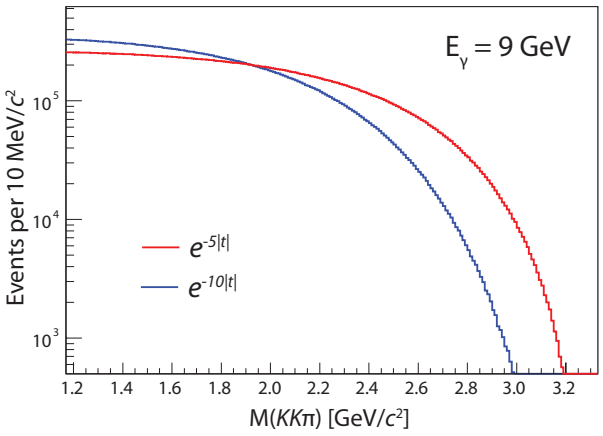

FIG. 9. A figure showing the number of expected events per 10 MeV/c^2 bin in $KK\pi$ invariant mass, integrating over all allowed values of t, and assuming 3×10^7 events in total are produced. No dependence on $M(KK\pi)$ is assumed, although, in reality, the mass dependence will likely be driven by resonances. Two different assumptions for the t dependence are shown. The region above 2.5 GeV/c^2 represents about 8% (2%) of all events for the $\alpha = 5(10)$ GeV^{-2} values.

the mass region where $s\bar{s}$ exotics are expected to reside. More importantly, it stresses the need to maximize the statistical precision of the data in order to be able to search for heavier exotic mesons.

Recent CLAS data for the $\Xi(1320)$ are consistent with t-slope values ranging from 1.11 to 2.64 $(\mathrm{GeV}/c)^{-2}$ for photon energies between 2.75 and 3.85 GeV [29]. Values for excited Cascades are not well known, but a recent unpublished CLAS analysis of a high-statistics data sample (JLab proposal E05-017) indicates that the t-slope value flattens out above 4 GeV at a value of about 1.7 $(\mathrm{GeV}/c)^{-2}$ [56]. We have used a value of 1.4 $(\mathrm{GeV}/c)^{-2}$ for the $\Xi^-(1320)$ and 1.7 $(\mathrm{GeV}/c)^{-2}$ for the $\Xi^-(1820)$ in our simulations at 9 GeV. For the reactions in Fig. 6, we estimate a detection efficiency of about 10%. The most recent CLAS analysis has determined a total cross section of about 8 nb and 2 nb for the $\Xi^-(1320)$ and $\Xi^-(1530)$, respectively, at $E_\gamma = 5$ GeV. The analysis shows that the total cross section levels out above 3.5 GeV, but the energy range is limited at 5.4 GeV [56]. A total number of about 20,000 $\Xi^-(1320)$ events was observed for the energy range $E_\gamma \in [2.69, 5.44]$ GeV. GlueX will collect over an order of magnitude more data: using Eq. (5), we expect about 400,000 $\Xi^-(1320)$ and 100,000 $\Xi^-(1530)$ events to be collected in Phase IV.

In summary, we request a production run consisting of 200 days beam time at an average intensity of 5×10^7 γ/s for production Phase IV running of the GlueX experiment. An additional 20 days of beam will be needed to commission the Phase IV detector hardware, with some time between the 20 day commissioning run and the 200-day Phase IV run to assess the results. It is anticipated that the Phase IV intensity will start around 10^7 γ/s, our Phase III intensity, and increase toward the GlueX design goal of 10^8 γ/s as we understand the detector capability for these high rates based on the data acquired at 10^7 γ/s. The data sample acquired will provide an order of magnitude improvement in statistical precision over the initial Phase II and III running of GlueX, which will allow a detailed study of high-mass states.

C. Level-three trigger

The energy spectrum of photons striking the target ranges from near zero to the full 12 GeV incident electron energy. For physics analyses, one is primarily interested in only those events in the coherent peak around 9 GeV, where there is a signal in the tagger that determines the photon energy. At a rate of 10^7 γ/s, the 120 μb total hadronic cross section at 9 GeV corresponds to a tagged hadronic event rate of about 1.5 kHz. Based on knowledge of the inclusive photoproduction cross section as a function of energy, calculations of the photon intensity in the region outside the tagger acceptance, and estimates for the trigger efficiency, a total trigger rate of about 20 kHz is expected. At a typical raw event size of 15 kB, the expected data rate of 300 MB/s will saturate the available bandwidth to disk – rates higher than 10^7 γ/s cannot be accommodated with the current data acquisition configuration.

For the high-intensity running, we propose the development of a level-three software trigger to loosely skim events that are consistent with a high energy γp collision. The events of interest will be characterized by high-momentum tracks and large energy deposition in the calorimeter. Matching observed energy with a tagger hit is a task best suited for software algorithms like those used in physics analysis. It is expected that a processor farm can analyze multiple events in parallel, providing a real time background rejection rate of at least a factor of ten. While the exact network topology and choice of hardware will ultimately depend on the speed of the algorithm, the system will need to accommodate the 3 GB/s input rate, separate data blocks into complete events, and output the accepted events to disk at a rate of < 300 MB/s. The software trigger has the added advantage of increasing the concentration of tagged γp collision events in the output stream, which better optimizes use of disk resources and enhances analysis efficiency.

A simple estimate indicates that the implementation of a level-three trigger easily results in a net cost savings rather than a burden. Assuming no bandwidth limitations, if we write the entire unfiltered high-luminosity data stream to tape, the anticipated size is about 30 petabytes per year[5]. Estimated media costs for storage of this data at the time of running would be \$300K, assuming that no backup is made. A data volume of this size would require the acquisition of one or more additional tape silos at a cost of about \$250K each. Minimum storage costs for a multi-year run will be nearing one million dollars. Conversely if we assume a level-three trigger algorithm can run a factor of ten faster than our current full offline reconstruction, then we can process events at a rate of 100 Hz per core. The anticipated peak high luminosity event rate of 200 kHz would require 2000 cores, which at *today's costs* of 64-core machines would be about \$160K. Even if a factor of two in computing is added to account for margin and data input/output overhead, the cost is significantly lower than the storage cost. Furthermore, it is a fixed cost that does not grow with additional integrated luminosity, and it reduces the processing cost of the final stored data set when a physics analysis is performed on the data.

[5] This is at the GlueX design intensity of 10^8 γ/s, which is higher than our Phase IV average rate of 5×10^7 by a factor of two; however, other factors that would increase the data volume, such as event size increases due to higher-than-estimated noise or the additional data size associated with a RICH detector, have not been included.

TABLE IV. A table of relevant parameters for the various phases of GlueX running.

	Approved			*Proposed*
	Phase I	Phase II	Phase III	Phase IV
Duration (PAC days)	30	30	60	220[a]
Minimum electron energy (GeV)	10	11	12	12
Average photon flux (γ/s)	10^6	10^7	10^7	5×10^7
Average beam current (nA)	50 - 200[b]	220	220	1100
Maximum beam emittance (mm·μr)	50	20	10	10
Level-one (hardware) trigger rate (kHz)	2	20	20	200
Raw Data Volume (TB)	60	600	1200	2300[c]

[a] Twenty days are dedicated to Phase IV hardware commissioning and will be scheduled in advance of the 200-day physics run.
[b] An amorphous radiator may be used for some commissioning and later replaced with a diamond.
[c] This volume assumes the implementation of the proposed level-three software trigger.

D. Phase IV hardware development plan

The collaboration has started a program to develop a detailed and final conceptual design for a forward particle identification system. As demonstrated, the existing GlueX software framework will permit a simulation of reactions of interest in addition to providing the capability to analyze the impact of additional detector material on existing calorimeter and tracking performance. The development of a kaon detector will be a multi-institutional effort. Currently, simulations of kaon production are being carried out at Florida State University. Jefferson Lab has contributed to optimization of the mirror design for the gas Cherenkov detector in addition to the conceptual development of the HBRICH. This year, Massachusetts Institute of Technology, a group that has experience with the RICH detector at LHCb, has joined the collaboration with the desire to take a lead role in the construction of a forward particle identification system. A workshop has been organized for May 2012 in order to develop a plan for moving towards a complete design. The collaboration has set a goal of converging on a design decision by the fall of 2012 so that an accurate cost estimate can be obtained. It is expected that key proponents within the collaboration will initially seek funding through appropriate NSF and DOE programs, *e.g.,* the NSF Major Research Instrumentation Program or the DOE Early Career Award Program, to fund the construction of the detector. It should be noted that the member institutions of GlueX have significant detector construction capabilities – most major detector systems have been constructed offsite at GlueX institutions. As construction of the baseline GlueX detector will be complete at the institutions by 2014, resources may be redirected to assist in the construction of a forward particle identification system.

The level-three trigger can largely be developed as proposed in the initial GlueX design. The present baseline data acquisition system has been carefully developed so that a level-three software trigger can be easily accommodated in the future. Given the standardized approach to data acquisition and networking in place at Jefferson Lab, the lab staff would have to play a key role in developing and deploying the level-three trigger. As noted above, at the GlueX design intensity of 10^8 γ/s, the operational cost of managing all of the data produced by the experiment will likely outstrip the one-time hardware cost associated with developing a level-three trigger.

VI. SUMMARY

In summary, we propose an expansion of the present baseline GlueX experimental program to include both higher statistics and the capability to detect kaons over a broad range of phase space. This detection capability would allow the identification of meson states with an $s\bar{s}$ component and the search for doubly-strange Ξ-baryon states. The program would require 220 days of beam time with 9 GeV tagged photons at an average intensity of 5×10^7 γ/s. The data taking will be divided into an initial twenty-day commissioning period for the Phase IV hardware and then a 200-day production Phase IV physics run. The Phase IV running will provide an increase in statistics over the approved Phase II and III GlueX runs by an order of magnitude. To execute this program, a new forward particle identification system will be developed in order to supplement the existing capability of the forward time-of-flight system. In addition, a level-three software trigger is needed to provide an order of magnitude reduction in the rate at which background photoproduction events are written to disk, which would allow the experiment to run efficiently at high intensity and minimize the final disk and tape resources needed to support the data. With these enhanced capabilities, GlueX will be able to conduct an exhaustive study of both $s\bar{s}$ and $\ell\bar{\ell}$ mesons, thereby providing crucial experimental data to test the quantitative predictions of hybrid and conventional mesons that are emerging from both lattice calculations and other models of QCD.

[1] J. J. Dudek, Phys. Rev. D **84**, 074023 (2011) [arXiv:1106.5515 [hep-ph]].

[2] GlueX Collaboration, "Mapping the Spectrum of Light Quark Mesons and Gluonic Excitations with Linearly Polarized Protons," *Presentation to PAC 30*, (2006). Available at: *http://www.gluex.org/docs/pac30_proposal.pdf*

[3] GlueX Collaboration, "The GlueX Experiment in Hall D," *Presentation to PAC 36*, (2010). Available at: *http://www.gluex.org/docs/pac36_update.pdf*

[4] J. J. Dudek, R. G. Edwards, M. J. Peardon, D. G. Richards and C. E. Thomas, Phys. Rev. Lett. **103**, 262001 (2009) [arXiv:0909.0200 [hep-ph]].

[5] J. J. Dudek, R. G. Edwards, M. J. Peardon, D. G. Richards and C. E. Thomas, Phys. Rev. D **82**, 034508 (2010) [arXiv:1004.4930 [hep-ph]].

[6] J. J. Dudek, R. G. Edwards, B. Joo, M. J. Peardon, D. G. Richards and C. E. Thomas, Phys. Rev. D **83**, 111502 (2011) [arXiv:1102.4299 [hep-lat]].

[7] R. G. Edwards, J. J. Dudek, D. G. Richards and S. J. Wallace, Phys. Rev. D **84**, 074508 (2011) [arXiv:1104.5152 [hep-ph]].

[8] J. J. Dudek and R. G. Edwards, Phys. Rev. D **85**, 054016 (2012) [arXiv:1201.2349 [hep-ph]].

[9] K. Nakamura *et al.* [Particle Data Group Collaboration], J. Phys. G G **37**, 075021 (2010).

[10] T. Aaltonen *et al.* [CDF Collaboration], Phys. Rev. Lett. **99**, 202001 (2007).

[11] V. M. Abazov *et al.* [D0 Collaboration], Phys. Rev. Lett. **99**, 052001 (2007).

[12] T. Aaltonen *et al.* [CDF Collaboration], Phys. Rev. Lett. **107**, 102001 (2011) [arXiv:1107.4015 [hep-ex]].

[13] V. M. Abazov *et al.* [D0 Collaboration], Phys. Rev. Lett. **101**, 232002 (2008).

[14] T. Aaltonen *et al.* [CDF Collaboration], Phys. Rev. D **80**, 072003 (2009).

[15] M. Ablikim *et al.* [BESIII Collaboration], Phys. Rev. Lett. **106**, 072002 (2011) [arXiv:1012.3510 [hep-ex]].

[16] G. S. Adams *et al.* [CLEO Collaboration], Phys. Rev. D **84**, 112009 (2011) [arXiv:1109.5843 [hep-ex]].

[17] E. I. Ivanov *et al.* [E852 Collaboration], Phys. Rev. Lett. **86**, 3977 (2001) [hep-ex/0101058].

[18] C. A. Meyer and Y. Van Haarlem, Phys. Rev. C **82**, 025208 (2010) [arXiv:1004.5516 [nucl-ex]].

[19] B. Aubert *et al.* [BABAR Collaboration], Phys. Rev. Lett. **95**, 142001 (2005) [hep-ex/0506081].

[20] T. E. Coan *et al.* [CLEO Collaboration], Phys. Rev. Lett. **96**, 162003 (2006) [hep-ex/0602034].

[21] Q. He *et al.* [CLEO Collaboration], Phys. Rev. D **74**, 091104 (2006) [hep-ex/0611021].

[22] C. Z. Yuan *et al.* [Belle Collaboration], Phys. Rev. Lett. **99**, 182004 (2007) [arXiv:0707.2541 [hep-ex]].

[23] J. J. Dudek and E. Rrapaj, Phys. Rev. D **78**, 094504 (2008) [arXiv:0809.2582 [hep-ph]].

[24] L. Liu *et al.*, arXiv:1204.5425 [hep-ph].

[25] B. Aubert *et al.* [BABAR Collaboration], Phys. Rev. D **74**, 091103 (2006) [hep-ex/0610018].

[26] M. Ablikim *et al.* [BES Collaboration], Phys. Rev. Lett. **100**, 102003 (2008) [arXiv:0712.1143 [hep-ex]].

[27] C. P. Shen *et al.* [Belle Collaboration], Phys. Rev. D **80**, 031101 (2009) [arXiv:0808.0006 [hep-ex]].

[28] J. W. Price *et al.* [CLAS Collaboration], Phys. Rev. C **71**, 058201 (2005).

[29] L. Guo *et al.*, Phys. Rev. C **76**, 025208 (2007) [arXiv:nucl-ex/0702027].

[30] Y. Van Haarlem *et al.*, Nucl. Instrum. Meth. A **622**, 142 (2010) [arXiv:1004.3796 [nucl-ex]].

[31] B. D. Leverington *et al.*, Nucl. Instrum. Meth. A **596** (2008) 327.

[32] A. Brunner *et al.*, Nucl. Instrum. Meth. A **414**, 466 (1998).

[33] G. S. Adams *et al.* [E852 Collaboration], Phys. Rev. Lett. **81**, 5760 (1998).

[34] A. R. Dzierba *et al.*, Phys. Rev. D **73**, 072001 (2006) [hep-ex/0510068].

[35] M. Alekseev *et al.* [COMPASS Collaboration], Phys. Rev. Lett. **104**, 241803 (2010) [arXiv:0910.5842 [hep-ex]].

[36] M. Nozar *et al.* [CLAS Collaboration], Phys. Rev. Lett. **102**, 102002 (2009) [arXiv:0805.4438 [hep-ex]].

[37] F. Haas, AIP Conf. Proc. **1374**, 273 (2011) [arXiv:1109.1789 [hep-ex]].

[38] P. R. Page, E. S. Swanson and A. P. Szczepaniak, Phys. Rev. D **59**, 034016 (1999) [hep-ph/9808346].

[39] N. Isgur, R. Kokoski and J. E. Paton, Phys. Rev. Lett. **54**, 869 (1985).

[40] F. E. Close and P. R. Page, Phys. Lett. B **628**, 215 (2005) [hep-ph/0507199].

[41] S. -L. Zhu, Phys. Lett. B **625**, 212 (2005) [hep-ph/0507025].

[42] E. Kou and O. Pene, Phys. Lett. B **631**, 164 (2005) [hep-ph/0507119].

[43] X. -Q. Luo and Y. Liu, Phys. Rev. D **74**, 034502 (2006) [Erratum-ibid. D **74**, 039902 (2006)] [hep-lat/0512044].

[44] G. -J. Ding and M. -L. Yan, Phys. Lett. B **657**, 49 (2007) [hep-ph/0701047].

[45] B. Aubert *et al.* [BABAR Collaboration], Phys. Rev. D **78**, 034008 (2008).

[46] S. F. Biagi *et al.*, Z. Phys. C **34**, 175 (1987).

[47] R. D. Tripp *et al.*., Nucl. Phys. B **3**, 10 (1967).

[48] G. Burgun *et al.*, Nucl. Phys. B **8**, 447 (1968).

[49] P. J. Litchfield *et al.*, Nucl. Phys. B **30**, 125 (1971).

[50] M. Iodice *et al.*, Nucl. Instrum. Meth. A **553**, 231 (2005) [Erratum-ibid. A **556**, 644 (2006)].

[51] W. Anderson *et al.*, Nucl. Instrum. Meth. A **646**, 35 (2011) [arXiv:1103.4277 [physics.ins-det]].

[52] F. Sauli, Nucl. Instrum. Meth. A **386**, 531 (1997).

[53] M. Alfonsi *et al.*, Nucl. Instrum. Meth. A **617**, 151 (2010).

[54] A. Pickford [LHCb RICH Collaboration], Nucl. Instrum. Meth. A **604**, 297 (2009).

[55] A. Baldini, V. Flaminio, W. G. Moorhead, D. R. O. Morrison and H. Schopper, (Ed.), "Numerical Data And Functional Relationships In Science And Technology. Grp. 1: Nuclear And Particle Physics. Vol. 12: Total Cross-sections For Reactions Of High-energy Particles (including Elastic, Topological, Inclusive And Exclusive Reactions). Subvol," BERLIN, GERMANY: SPRINGER (1988) 409 P. (LANDOLT-BOERNSTEIN. NEW SERIES, 1/12B)

[56] John Theodore Goetz, Ph.D. Thesis, University of California, Los Angeles, 2010 (unpublished).